Natural Resources Research, Vol. 17, No. 2, June 2008 (© 2008)
DOI: 10.1007/s11053-008-9069-6

Mineral Potential Modelling for the Greater Nahanni Ecosystem Using GIS Based Analytical Methods

J. R. Harris,[1,4] D. Lemkow,[1] C. Jefferson,[2] D. Wright,[2] and H. Falck[3]

Received 15 December 2007; accepted 25 April 2008
Published online: 28 May 2008

Mineral potential within the Greater Nahanni Ecosystem (GNE) was modelled in a Geographic Information System (GIS) for four different deposit types: (1) SEDEX (stratiform shale-hosted sedimentary exhalative Zn–Pb–Ag), (2) 'Carbonate-Fault' (carbonate-hosted zinc–lead–silver associated with major faults), (3) 'Intrusion-Related' (includes skarn, rare metals and gemstones) and (4) Carlin-Type gold as lode and/or derived placer deposits. This mineral potential modelling study integrates data collected during the Nahanni Mineral and Energy Resource Assessment (MERA) undertaken from 2003 to 2007. The results have contributed to the process of determining the geographic boundaries of the proposed expansion of the Nahanni National Park Reserve. Four mineral potential maps were produced (one for each deposit type) using a knowledge-driven approach. A weighting scheme based on integrated mineral deposit and regional geological knowledge was derived for the various evidence maps for each deposit model using expert opinion. The four potential maps were then combined into a final potential map using a maximum operator. Plots showing the efficiency of the models (mineral potential maps) for predicting the known occurrences of the four deposit types show that partial data sets provide reasonable predictions of the remaining known mineral prospects, occurrences and deposits. Hydrocarbon potential from Nahanni MERA 1 was added to the final potential map to ensure that both mineral and energy potential data were incorporated into the park configuration modelling.

KEY WORDS: GIS, spatial modelling, mineral potential, Nahanni, MERA.

INTRODUCTION

This article documents the application of a GIS (Geographic Information System)-based on a knowledge-driven approach to model mineral potential within the Greater Nahanni Ecosystem (GNE) using one single and three composite deposit models: (1) SEDEX (stratiform shale-hosted sedimentary-exhalative Zn–Pb–Ag), (2) 'Carbonate-Fault' (carbonate-hosted base-metals associated with major faults), (3) 'Intrusion-Related' (includes skarn, rare metals and gemstones) and (4) 'Carlin-Type' gold as lode and/or derived placer. The composite models are not formally recognized deposit types in the literature, but are informal amalgamations of several deposit types used specifically for this resource assessment, because their component types have so many attributes in common. They are capitalized throughout for ease of recognition by the reader, and defined in the DEPOSIT MODELS section later.

This work was carried out as part of the formal Mineral and Energy Resource Assessment (MERA) process (Government of Canada, 1995). An initial MERA (referred to herein as MERA 1) was conducted for two smaller regions adjacent to the existing Nahanni National Park Reserve between

[1]Geological Survey of Canada, 615 Booth St., Ottawa ON, Canada K1A 0E9.
[2]Geological Survey of Canada, 601 Booth St., Ottawa ON, Canada K1A 0E8.
[3]Northwest Territories Geoscience Office, 4601-B 52nd Ave., Yellowknife, Canada NT X1A 2R3.
[4]To whom correspondence should be addressed; e-mail: harris@nrcan.gc.ca

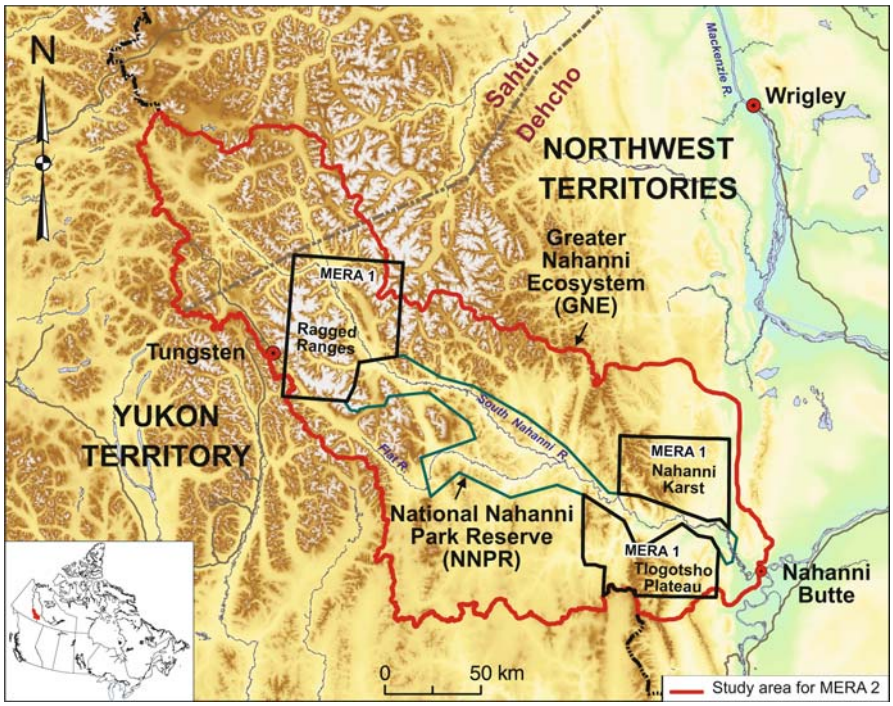

Figure 1. Index and regional geographic context of Nahanni MERA 2 study area. MERA 1 study areas were: Nahanni Karst, Ragged Ranges and Tlogotsho Plateau.

1985 and 1988 (Jefferson and Spirito, 2003). MERA 2, conducted from 2003 to 2007 covers an expanded region including the entire catchment for the Nahanni River (Fig. 1).

The GIS analysis was undertaken with the purpose of producing mineral potential maps as systematically and quantitatively as possible from the suite of mineral-related studies completed under MERA 1 and MERA 2. The relative potential is estimated for the study area only, and there is no intent in this article to imply absolute values of potential for undiscovered mineral resources. The results generated from the GIS mineral deposit modelling were transferred to Parks Canada for use in their GIS modelling related to defining park boundary options.

Mineral Potential Modelling Methods

Numerous modelling methods for producing mineral potential maps using a GIS have been developed over the past 20 years. These methods can be divided into two basic categories: data-driven and knowledge-driven techniques, for which reviews can be found in Bonham-Carter (1994) and Wright and Bonham-Carter (1996). A knowledge-driven approach was used in this study because only one producing mine (Canada Tungsten) is present in the study area. This is not a sufficient training set to enable a data-driven approach. This knowledge-driven technique consists of a simple weighting system in which each type of evidence for each mineral potential model was assigned a relative weight (reflecting importance) ranging in value from 1 to 10. This is based on expert opinion of the third and fifth authors of this article and their exploration knowledge of the area.

Data-driven methods make use of the location of mineral deposits with respect to individual evidence maps to derive the weights for each evidence map (Bonham-Carter, 1994, ch. 9). In this study, the location of mineral occurrences of a given deposit type were divided into four classes (defined resources, advanced prospect, showing and anomaly), assigned a weight and incorporated as evidence maps in the modelling process. Thus information on mineral occurrences was incorporated in the modelling process albeit using a different strategy than that used for data-driven approaches.

Hydrocarbon resource potential was not specifically assessed in the Nahanni MERA 2 but has

been assessed by Osadetz, Chen, and Morrow (2003). Three areas (see later figure) with significant hydrocarbon potential within the GNE were identified in the southeast portion of the study area: Twisted Mountain Anticline, Mattson Anticline and the Etanda Dome. A hydrocarbon potential map was constructed comprising these three areas and converted to a binary map in which all three areas were given a high weight based on exploration knowledge (Osadetz, pers comm., 2007).

Particular weight was given to evidence derived from the studies supported by Nahanni MERA 2 that focussed on significant local mineral occurrences and are reported in Barnes, Groat, and Falck (2007), Charbonneau (2007), Cousens (2007), Paradis (2007), Rasmussen and others (2007), and Yuvan, Shelton, and Falck (2007).

The assessment process used in this study employs GIS quantitative spatial analysis techniques to produce semi-quantitative relative mineral potential maps. This differs from all previous MERA studies which employed a completely subjective and much less systematic ''light table'' approach whereby analogue maps were overlaid and judged with respect to mineral potential. A powerful asset of the new GIS approach is to provide direct input to the GIS-based park planning system that does a cost-benefit analysis of biotic, physiographic and ecosystem attributes of importance to modern park sustainability to develop boundary options for public consultation purposes.

Study Area

The area being assessed for this study is located in the southwestern corner of the Northwest Territories (Fig. 1). It includes the entire length and catchment area of the South Nahanni River and a small extension to the northeast that includes the Ram Plateau. This assessment area is known as the GNE. It is approximately 400 km long and 150 km across, from latitude 63°00′ to 60°45′N and from longitude123°50′ to 129°45′W. The total area of the GNE is approximately 39,000 km^2. In this assessment the existing Nahanni National Park Reserve was excluded from the area of data collection, therefore the additive modelling process automatically produces an artificially depressed mineral potential within its boundaries. Data from the areas assessed in the MERA 1 study collected between 1985 and 1988 (Jefferson and Spirito, 2003) were integrated into this GIS study to provide seamless mineral potential maps throughout the balance of the GNE.

Geological Setting

In paleogeographic terms, this region was situated on the western margin of the North American Craton from more than 800 million years ago until the Middle Devonian, about 350 million years ago. Along this margin, the sedimentary rocks of the western two-thirds of this region were deposited in the shaly, deep-marine Selwyn Basin, whereas the eastern third of the strata are shallow marine carbonate shelf facies of the MacDonald Platform. After the Middle Devonian, conglomerate and black shale were derived from colliding terranes to the west and silty shale was derived from distal orogens to the east. These two different shale successions were roughly coeval and their interface in the central part of the study area is poorly known. The western part of the study area was uplifted due to continued mountain building in the west, and a mixture of foreland shale, limestone, and coal-bearing sandstone were deposited in the southern and eastern areas.

The next geological phase of this region was dominated by structural and igneous activity. The Mackenzie Mountains were produced by compressional folding and thrusting of the above sedimentary units during the Jurassic (~170 Ma) to Cretaceous (~100 Ma). Major granitoid batholiths (Selwyn Plutonic Suite) intruded these rocks during a Cretaceous collision of an island arc with western North America. The majority of the plutons are quartzofeldspathic and have accessory minerals within a narrow range of compositions that permit the plutons to be classified as biotite-muscovite ('two-mica'), biotite-hornblende or biotite (Gordey and Anderson, 1993; Rasmussen and others, 2007). Right-lateral strike-slip motion along major faults began in the Tertiary (~40 Ma) and continues today.

The present landscape and exposed rock units (Fig. 2) are a result of recent weathering and erosion by water and ice during and after tectonic uplift. The eastern section of the study area is a dissected plateau exposing broadly folded karst (vertical dissolution of carbonate rocks by rain water produced sinkholes and caves) on the north side of the Nahanni River and coal-bearing sandstone and shale with minor limestone on the south side. Continental

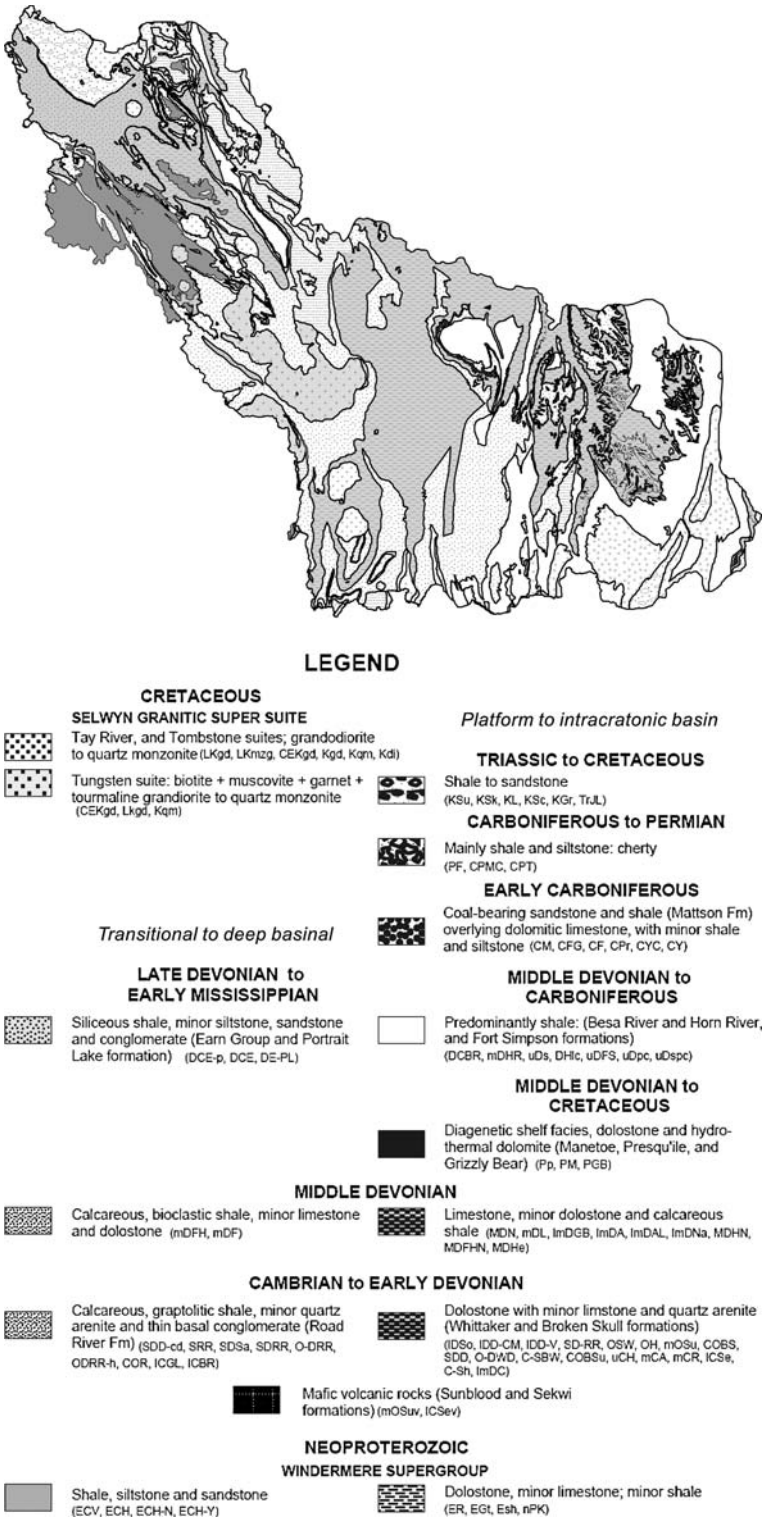

Figure 2. Geology used for spatial modelling of Nahanni MERA 2 study area, after Jefferson and Spirito (2003), Okulitch (2005a, 2005b) and Rasmussen and others (2007). Units are combined in different ways (favourite rock units) for different mineral deposit models as listed in Tables 1–4.

glaciers carried till and mud east from the Canadian Shield into the eastern part of the study area. Mountain glaciers carved the U-shaped valleys and cirques into the Selwyn Ranges (Duk-Rodkin, Huntley, and Smith, 2007). More details on the geology of the study area are provided by Jefferson, Spirito, and Hamilton (2003), Okulitch (2005a, in review) and Falck (2007).

Data Collection

A critical component of the Nahanni MERA was to compile existing data in addition to data collected during the MERA 2 project into a digital, georeferenced GIS database. A comprehensive digital database covering the entire study area is essential to conduct the MERA and mineral potential modelling using GIS-based analytical methods. In total the current GIS database contains over 200 layers of digital geoscience data including bedrock geology, surficial geology, geochemistry, geophysics, mineral deposits and topographic data (Lemkow, Harris, and Slack, 2007).

A selection of the bedrock geology compiled by Okulitch (2005b; 2005a, in review) at a scale of 1:1,000 000 is included in the digital GIS database. The bedrock geology map (Fig. 2) is a simplified classification of the major bedrock lithological groupings based on Okulitch (2005a). This fundamental framework locates key geological attributes associated with the four deposit models that in turn embrace the most likely deposit types to be found in the study area. These lithologic attributes include primary sedimentary rock types, products of diagenetic alteration (e.g. Manetoe facies; Morrow, Cumming, and Aulstead, 1990), structure (faults and folds) and intrusive rock types (granitic plutons). All of these lithologic attributes provide indirect evidence for sources, transport and deposition of elements that may have formed mineral deposits.

A total of 2,463 stream sediment samples and 2,068 stream water samples were collected (Fig. 3a) by various surveys within the GNE and geochemically

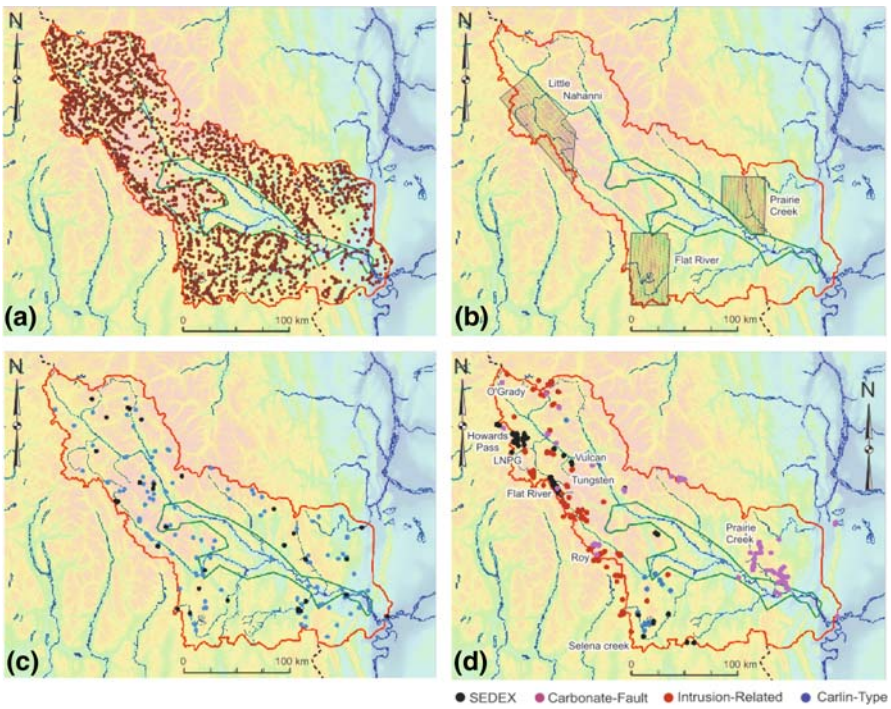

Figure 3. Locations of data collected for Nahanni MERA 1 and 2. (a) Locations of stream sediment and water samples collected by Spirito and Jefferson (2003) in MERA 1 areas and by McCurdy and others (2007) for MERA 2 under National Geochemical Reconnaissance (NGR) programme. (b) Locations of geophysical surveys as reported by Charbonneau (2007). (c) Locations of spring water sample sites, from Hamilton and others (2003) for MERA 1 areas, and from Caron, Grasby, and Ryan (2007). Anomalous springs are shown by black dots. (d) Locations of mineral occurrences from NORMIN.db. Deposit models are explained in text.

analyzed to help model mineral potential. Over half these samples (1,374 stream sediment and 1,378 stream water samples) were collected by McCurdy and others (2007) as part of MERA 2 during the 2004 and 2005 field seasons and combined with additional geochemical data for stream sediments and waters from previous surveys: 396 sediment samples from the first Nahanni MERA (Jefferson and Spirito, 2003); 693 sediment samples and 683 water samples from previous National Geochemical Reconnaissance surveys (Friske, McCurdy and Day, 2001; Day and others, 2005). All of these data are included in the GIS database and were spatially analyzed herein.

Detailed public domain airborne geophysical data were not available for the study area prior to this MERA study. Therefore, as part of the Nahanni MERA 2 project, three airborne surveys were flown at 135 m nominal terrain clearance along lines spaced at 500 m for a total of 16,000 line kilometres over three areas shown in Fig. 3b. These areas were considered most likely to generate conflicts between mineral potential and other competing land uses. The geophysical data provide additional evidence to help build the mineral deposit knowledge base, refine the mineral potential modelling, and may help resolve future planning issues. For each area, ten themes of data were generated including total radioactivity, potassium (K%), equivalent uranium (eU, ppm), equivalent thorium (eTh, ppm), eU/eTh, eU/K, eTh/K, ternary radioactive plots (K, eU, eTh), residual magnetic total field (nT), and calculated magnetic vertical gradient (nT/m). Key aspects of these surveys are discussed and illustrated by Charbonneau (2007). The full primary data sets have been published (Carson and others, 2007a, 2007b, c) and are included in the GIS database (Lemkow, Harris, and Slack, 2007).

Spring water geochemistry can be an effective tool for investigating regional compositional trends and for indirectly detecting buried mineral deposits that were transected by sub-terranean flow paths. Spring water geochemistry surveys reported by Hamilton and others (2003) and Caron, Grasby, and Ryan (2007) contributed to the Nahanni MERA 1 and MERA 2, respectively. A total of 95 samples (Fig. 3c) collected from 78 springs for those studies were compiled and integrated for this GIS analysis.

Mineral deposit data (Fig. 3d) were compiled and rationalized for the Nahanni MERA 1 over the entire watershed (Jefferson and Spirito, 2003). This data, a significant contribution to the NORMIN database (Department of Indian Affairs and Northern Development, 2006), was augmented by mineral deposit studies conducted as part of the Nahanni MERA 2 (Rasmussen, Mortensen, and Falck, 2006; Paradis, 2007; Barnes, Groat, and Falck, 2007; Cousens, 2007; Yuvan, Shelton, and Falck, 2007, Rasmussen and others, 2007). All known mineral showings in the study area as determined from the NORMIN database and the current MERA study were classified into the four deposit models outlined in the following section.

DEPOSIT MODELS

Four different deposit models were designed to incorporate the most important mineral deposit types for this region (Fig. 3d), using the minimum number of GIS operations. The SEDEX (stratiform sediment-hosted exhalative Zn–Pb–Ag) model is a single deposit type that is well documented and pre-eminent in the region. The three other models are composites of two or more deposit types with spatial and genetic affinities, Carbonate-Fault Type, Intrusion-Related Type and Carlin-Type gold (Carlin or other types of intrusion-related lode gold and/or derived placer deposits). Each of these models is reviewed as follows.

SEDEX (Stratiform Sediment-Hosted Exhalative Zn–Pb–Ag)

The SEDEX mineral potential map created in this study is based on a well-known set of attributes summarized by Carne and Cathro (1982), Lydon (1995), Goodfellow (2007), and Cousens (2007). These include favourable host lithology (black, graphitic, siliceous shale with rapid lateral facies changes including conglomerate tongues), structural features (known faults, and faults inferred from facies changes), as well as direct and indirect pathfinder elements that are detected by stream sediment, stream water and spring water geochemistry surveys, and the locations of SEDEX-type mineral occurrences (Table 1).

SEDEX deposits are most likely to occur within the early Cambrian to Middle Devonian Selwyn Basin that comprises the deep-water euxinic (oxygen-poor) portions of the western North American passive margin sedimentary sequence. Two main districts at Macmillan Pass and Howard's Pass are defined by linear belts of such occurrences near the margins of

Table 1. The *SEDEX* mineral potential map created in this study is based on a well-known set of attributes summarized by Carne and Cathro (1982), Lydon (1995), Goodfellow (2007), and Cousens (2007)

	Weight
Favourable rock units	
1. Transitional to deep basinal strata (Cambrian to Early Devonian + Middle Devonian to Early Mississippian are established producers)	10
2. Basinal Windermere strata (theoretical producing rock package)	3
Structural features	
3. Cambrian and Ordovician volcanic units (like fault, represents deep crustal structure favouring hydrothermal fluid flow)	10
4. Volcanic: 10 km buffer outside units	3
5. Growth faults (north-northwesterly faults along Broken Skull River and parallels, parallels to the carbonate-shale facies change (#5), and parallels to the northeasterly Leith Ridge and Fort Norman structures are interpreted as Laramide expressions of deep crustal weaknesses by steeply dipping breaks discordant to regional fold and thrust trends): 3 km buffer	2
6. Carbonate-shale facies change (Ordovician-Devonian platform edge from Morrow, represents depositional structure favourable for SEDEX): 3 km buffer	2
7. All other faults (mainly southwest-dipping thrusts): 2 km buffer	1
Geochemistry; anomalous direct and indirect pathfinder elements	
8. Stream sediment, direct: Ag, Cu, Pb, Zn. (each element map was normalized (to provide equal influence) and then all elements were summed and the mean value was calculated—this map was divided into a five class map reflecting high to low concentration—class thresholds based on natural breaks in the data histogram)	10, 7, 2, 1, 0 by class
9. Stream sediment, indirect: As, Ba, Bi, Cd, Cr, F, Hg, Mn, Mo, Ni, P, Sb, V) (each element map was normalized (to provide equal influence) and then all elements were summed and the mean value was calculated—this map was divided into a five class map reflecting high to low concentration—class thresholds based on natural breaks in the data histogram)	6, 4, 2, 1, 0 by class
10. Stream water, direct: Ag, Cu, Pb, Zn. (each element map was normalized (to provide equal influence) and then all elements were summed and the mean value was calculated—this map was divided into a five class map reflecting high to low concentration—class thresholds based on natural breaks in the data histogram)	10, 7, 2, 1, 0 by class
11. Stream water, indirect: As, Ba, Cd, Cr, F, Mn, Mo, Ni, P, pH, Sb, V (each element map was normalized (to provide equal influence) and then all elements were summed and the mean value was calculated—this map was divided into a five class map reflecting high to low concentration—class thresholds based on natural breaks in the data histogram)	6, 4, 2, 1, 0 by class
12. Spring-water sample sites: all SEDEX from Table 5.12 of Hamilton and others, 2003 and selected springs from Table 6 of Caron, Grasby, and Ryan, 2007) anomalous in one or more of 14 pathfinder elements: direct: Ag, Cu, Pb, Zn; and indirect: As, Ba, Cd, Cr, Mn, Mo, Ni, pH, Sb, V. buffer = 3 km.	2
13. Ph—sampled from water chemistry—data were interpolated and map divided into eight classes reflecting acid to basic conditions	10, 9, 8, 7, 4, 3, 2, 0
14. Mineral occurrences of the SEDEX type were assigned to one of 4 categories: defined resources (weight 10), advanced prospect (weight 7), showing (weight 4), anomaly (weight 2). Buffer = 3 km.	10, 7, 4, 2

TOTAL of 17 evidence maps used for producing the SEDEX potential map

Explanatory notes for Tables 1–4 inclusive:

- Anomalous cut-offs were determined by separate statistical analysis of frequency distribution of results for samples in each of the rock units used for each deposit model
- The 'Buffer' for each sample is calculated by interpolation within a data-determined zone of influence
- Each sample location is assigned to a rock unit based on straightforward spatial intersection. Although most individual stream catchment areas and spring water flow paths intersect multiple rock types, their relative proportions were NOT taken into account in determining the background rock influence on each sample. In a few cases, the location is just inside a rock unit that did not contribute significantly to the sample medium
- Stream water pH data were included in stream sediment geochemistry as well as stream water geochemistry for spatial modelling (see discussion in text under SEDEX)

the Selwyn Basin. The only past-producing SEDEX deposits in the Selwyn Basin are those of the Anvil District hosted by basal Cambrian shay strata near Whitehorse. The deposits in the Howard's Pass district contain some of the largest base metal accumulations in the world.

Carbonate-Fault

Favourable rock units, structural features, geochemistry and the location of Carbonate-Fault-associated mineral occurrences (Table 2) were used to produce a mineral potential map.

Table 2. "*CARBONATE—FAULT*" (3 spatially associated types of zinc–lead–silver massive sulphide: stratabound, Mississippi Valley and vein quartz-carbonate of the Prairie Creek camp as summarized by Paradis, 2007)

	Weight
Favourable rock units	
1. Diagenetic Facies (vuggy recrystallized dolostone of the Devonian to Cretaceous Manetoe (PM), Presqu'ile (Pp) and Grizzly Bear (PGB) formations)	10
2. Middle Devonian (all strata: limestone, dolostone and shale)	5
3. Cambrian to Early Devonian Platformal (limestone and dolostone)	5
4. Cambrian to Early Devonian Transitional to Deep Basinal (shale)	2
5. Buffer around Diagenetic Facies: 3 km buffer only in #3 to 5	5
Structural features	
6. Growth faults (as for SEDEX): 3 km buffer	2
7. Carbonate-shale facies change (as for SEDEX): 3 km buffer	2
8. All other faults (as for SEDEX): 2 km buffer	1
Geochemistry; anomalous direct and indirect pathfinder elements	
9. Stream sediment, direct: Ag, Cu, Pb, Zn (each element map was normalized (to provide equal influence) and then all elements were summed and the mean value was calculated—this map was divided into a five class map reflecting high to low concentration –class thresholds based on natural breaks in the data histogram)	10, 7, 2, 1, 0 by class
10. Stream sediment, indirect: Cd, F, Hg, Sb (each element map was normalized (to provide equal influence) and then all elements were summed and the mean value was calculated—this map was divided into a five class map reflecting high to low concentration—class thresholds based on natural breaks in the data histogram)	6, 4, 2, 1, 0 by class
11. Stream water, direct: Ag, Cu, Pb, Zn. (each element map was normalized (to provide equal influence) and then all elements were summed and the mean value was calculated—this map was divided into a five class map reflecting high to low concentration—class thresholds based on natural breaks in the data histogram)	10, 7, 2, 1, 0 by class
12. Stream water, indirect: Cd, F, Sb. (each element map was normalized (to provide equal influence) and then all elements were summed and the mean value was calculated—this map was divided into a five class map reflecting high to low concentration—class thresholds based on natural breaks in the data histogram)	6, 4, 2, 1, 0 by class
13. Spring-water sample sites: Prairie Creek mine water from Table 5.12 of Hamilton and others, 2003 and selected anomalous springs from Table 6 of Caron, Grasby, and Ryan, 2007) anomalous in one or more of 6 pathfinder elements: direct: Ag, Cu, Pb, Zn and indirect: Cd and Sb. Buffer = 3 km.	2
14. Mineral occurrences of the CARBONATE-FAULT type were assigned to one of 4 categories: defined resources (weight 10), showing (weight 4); buffer = 3 km.	10, 4
TOTAL of 15 evidence maps used for producing the CARBONATE—FAULT potential map	

The composite Carbonate-Fault deposit model accounts for the spatial association of zinc–lead–silver deposits of at least three types: (1) vein quartz-carbonate, (2) SEDEX and, (3) Mississippi Valley. Fluids trapped during sedimentation combined with fluids derived from deeply buried basement rocks may have leached metals from basement rocks as they flowed along more permeable zones, driven by pressure due to increased burial near basin centres, by differential tectonic uplift or subsidence, or by thermal convection. Where the fluids encountered fault zones in competent rocks, the permeability was locally enhanced, thereby focussing the fluids. As these fluids passed through other layers including different aquifers, reaction with the wall rock or mixing with fluids from other aquifers may have altered the parameters of the fluid sufficiently for metals to precipitate. The Manetoe digenetic alteration facies (Morrow, Cumming, and Aulstead, 1990) is an example of the alteration of carbonate layers due to basinal fluids. Mississippi Valley-type base-metal deposits (MVT) such as the classic past-producing Pine Point district are typically associated with this style of alteration. Faults especially reactivated vertical growth-faults, locally facilitated fluid transportation and mixing at Pine Point, as well as in variants of MVT, such as the Irish-type of carbonate-hosted Zn–Pb–Ag deposits. Faults may also have allowed great fluctuations in fluid pressure regimes, allowing the formation of breccias, stockworks and veins.

Intrusion-Related (Includes a Variety of Skarn, Rare Metal and/or Gemstone Types)

Favourable host lithology, distance to plutons of various types, structural features, favourable pathfinder elements in stream sediments, stream waters, and springs, and the locations of Intrusion-Related mineral occurrences (Table 3) were used to produce an Intrusion-Related potential map.

Table 3. *INTRUSION (Pluton)—RELATED*: skarn tungsten or zinc–lead–silver, rare metals and/or gemstones (excludes Carlin Gold), modelled after Dawson and others (1992), Barnes, Groat, and Falck (2007), Rasmussen and others (2007), and Yuvan, Shelton, and Falck (2007)

	Weight
Favourable rock units	
1. High-to very high potential granitic bodies (include hornfels): 1, 5 and 20 km buffers; weights 10, 5 and 2, respectively (inside and outside of margins only)	10, 5, 2
2. Moderate potential granitic bodies (include hornfels): 1, 5 and 10 km buffers; weights 5, 2 and 1, respectively (inside and outside of margins only)	5, 2, 1
3. Low potential granitic bodies: 1 and 5 km buffers, weights 3 and 1, respectively	3, 1
4. Shaly limestone units. Sedimentary units within a 20 km buffer of all granite bodies are weighted 1 to 10 for SKARN potential based on the presence of impure limestone units, with the #10 rank going to heterogeneous units (Vampire and Sekwi). Sedimentary unit values are added to the buffer values of the respective plutons	
Structural features	
5. Fault density map based on line density algorithm (assigned weights based on low, medium and high fault density)	5, 3, 1
Geochemistry	
6. Stream sediment, direct: Cu, Pb, W, Zn (each element map was normalized (to provide equal influence) and then all elements were summed and the mean value was calculated—this map was divided into a five class map reflecting high to low concentration—class thresholds based on natural breaks in the data histogram)	10, 7, 2, 1, 0 by class
7. Stream sediment, indirect: Ag, As, Au, Bi, Sb, Sn, Te. (each element map was normalized (to provide equal influence) and then all elements were summed and the mean value was calculated—this map was divided into a five class map reflecting high to low concentration—class thresholds based on natural breaks in the data histogram)	6, 4, 2, 1, 0 by class
8. Stream water, direct: Cu, Pb, W, Zn. (each element map was normalized (to provide equal influence) and then all elements were summed and the mean value was calculated—this map was divided into a five class map reflecting high to low concentration—class thresholds based on natural breaks in the data histogram)	10, 7, 2, 1, 0 by class
9. Stream water, indirect: Ag, As, Au, Bi, Sb, Sn, Te (each element map was normalized (to provide equal influence) and then all elements were summed and the mean value was calculated—this map was divided into a five class map reflecting high to low concentration—class thresholds based on natural breaks in the data histogram)	6, 4, 2, 1, 0 by class
10. Spring-water sample sites: three 'tungsten skarn' from Table 5.12 of Hamilton and others, 2003 and selected springs from Table 6 of Caron, Grasby, and Ryan (2007) anomalous in one or more of 6 direct pathfinder elements: W, Cu, Pb, Zn; and 8 indirect: Ag, As, Au, Bi, F, Sb, Sn, Te. Buffer = 3 km.	2
11. Mineral occurrences of the INTRUSION type (after Rasmussen and others 2007 and NORMIN, 2007) were assigned to one of 4 categories: defined resources (weight 10), advanced prospect (weight 5), showing (weight 2), anomaly (weight 1). Buffer = 3 km.	10, 5, 2, 1
TOTAL of 14 evidence maps used for producing the INTRUSION potential map	

Intrusions provided both primary metaliferous fluids and heat for metal redistribution and reconcentration. In addition to mineral concentrations which are direct products of the magma (rare element-bearing pegmatites and gemstones) the introduction of magmatic and meteoric fluids driven by heat energy from the intrusion and their interaction with reactive host rocks can produce many different styles of mineral deposits. These include the extensive skarn family, mantoe, chimney, epithermal, endoskarn, porphyry and high temperature replacement deposits. A wide range of metal assemblages and rare metals is associated with the Intrusion-Related family of deposits, including one or more of W, Cu, Zn, Pb, Ag, Au, As, Sb, Li, Ta, Cs and Sn (refer to Barnes, Groat, and Falck, 2007). For this Nahanni MERA 2 GIS analysis, gold (Au) is treated separately as described in the next section.

In order to form intrusion-associated metal concentrations a number of additional factors are important, to optimize the effects of heat energy and chemical reactions with host rocks. Fluid pathways are essential to channel fluids through and away from metal sources and focus them in zones where the deposition of metals can build up economic concentrations. Since the plutons intruded deformed sedimentary rocks, such pathways were generally along pre-existing structures (faults, fold axes and permeable strata) that may also have constrained the upward ascent of magma to form the intrusions.

Another critical aspect of these deposits is that the focussing parameters under which metals are

carried in solution must have changed in order to form an ore deposit rather than disperse the metals distally from the source and dilute them. Mechanisms to focus precipitation include chemical reaction with the wall rock (such as changes in pH (acidity), Eh (oxidation), trace element contents, cooling of the fluid and/or depressurization). For example, a hot, acidic, high-pressure fluid passing through a carbonate unit will be cooled and neutralized. This explains why limestone, dolomite, and calcareous shale layers are common hosts to skarn. Skarn deposits tend to be best developed in the first relatively pure limestone layer in a mixed stratigraphic assemblage that the hydrothermal fluids encounter on their ascent from the related intrusion.

Depressurization of mineralizing fluid related to an active fault system can also be important; thus the presence of faults as a transport mechanism and a concentration mechanism is also an important factor for localizing intrusion-related deposits. Ponding due to physical ''traps'' may also concentrate metals as the movement of fluids is impeded giving them time to cool.

Some deposits are located within a pluton, caused by ingress of fluid from country rock, concentrating alteration within the upper portion of the pluton (termed endoskarn). Endoskarn may be recognised by the presence of metamorphosed remnants of wall rock preserved in the pluton as roof pendants. Such alteration introduces more potassium into the pluton resulting in crystallization of potassic feldspar, muscovite and/or sericite clay, and registered by high K/U, and K/Th ratios. Gamma ray spectrometer data is useful for detecting potassium enrichment, and thereby targetting alteration associated with such deposits. Gamma ray data were acquired in three strategic areas located in Fig. 3b and interpreted as reported by Charbonneau (2007). The gamma ray data (K channel) were used as signature of potassic alteration.

Skarn deposits in the Canadian Cordillera are abundant, diverse and economically significant. In the study region skarn occurrences are localised where the Middle Cretaceous Selwyn Plutonic Suite discordantly intrudes the lowest and/or thickest limestone unit of an upper Proterozoic to lower Paleozoic shelf-carbonate pelite sequence. The broad thermal aureole at the contact between a Cretaceous quartz monzonite stock and a Lower Cambrian limestone unit is the setting of the world-class Cantung Mine. A belt of W, Cu (Zn, Mo) skarn showings to deposits follows an arcuate trend of generally small mid Cretaceous granitoid plutons from the southwestern Northwest Territories to the Dublin Gulch District of the Yukon Territory. This trend contains some of the largest and highest grade resources of skarn tungsten in the world, mainly in the Cantung Mine and in the Mac Tung deposit at Macmillan Pass. Thus proximity to a pluton, especially where in contact with an appropriate carbonate unit, is an important vector for Intrusion-Related deposits.

Carlin-Type (Intrusion- or Fault-Associated Lode Gold and/or Related Placer Deposits)

Favourable rock units, structural features, favourable stream sediment, stream water and spring water geochemistry, potassium anomalies detected by airborne gamma ray spectrometer data and the locations of intrusion-associated placer and lode gold mineral occurrences (Table 4) were used to produce a Carlin-Type mineral potential map.

Carlin-Type gold is a special, possibly Intrusion-Related deposit model that for this study comprises at least two basic genetic hypotheses. Recent research has determined many of the associated empirical factors involved in these highly economic and commonly very large gold deposits (Poulsen, 1996; Cline and others, 2005; Emsbo and others, 2006). The characteristics of these gold deposits range from stratiform disseminations, breccia zones, sinters and vein stockworks to bonanza-style vein systems. Richards (1989) and Rowan (1989) recognized some of the geochemical attributes of such deposits in the Selena Creek area. Work under MERA 2 reported by McCurdy and others (2007) and Charbonneau (2007) focussed on this area to further test the premise that As, Sb, Hg, Ti +/− Ba bearing placer-gold occurrences here were derived from one or more Carlin-Type lode-gold deposits.

Depending on the deposit being examined, the genesis of Carlin-Type gold has been ascribed to a number of different mechanisms. The varied appearances and settings of the different deposits have resulted in a range of hypotheses describing their possible origins, and these are summarized here by two generalized hypotheses. The first hypothesis emphasizes the common proximity of the deposits to granitoid intrusions (plutons) which are considered to have been the thermal engines that drove fluid flow and were themselves the source for much of the fluid that carried the gold and associated trace metals.

Table 4. *CARLIN &/or PLACER*: Intrusion-related lode gold and associated placer deposits (after Cline and others, 2005; Emsbo and others, 2006)

	Weight
Favourable rock units	
1. High-to very high potential granitic bodies (include hornfels): 1, 5 and 20 km buffers; weights 10, 5 and 2, respectively (inside and outside of margins only)	10, 5, 2
2. Moderate potential granitic bodies (include hornfels): 1, 5 and 10 km buffers; weights 5, 2 and 1, respectively (inside and outside of margins only)	5, 2, 1
3. Low potential granitic bodies: 1 and 5 km buffers, weights 3 and 1, respectively.	3, 1
4. Reactive limestone units. Carlin uses same sedimentary units and additive weighting as for SKARN	
Structural features (Hydrothermal flow corridors)	
5. Growth faults as for SEDEX, within 20 km of granite bodies, treat as vertical: 2 km buffer each side	1
6. All other faults, within 20 km of granite bodies 2 km buffer down dip to SW	1
7. Fault intersections, within 20 km of granite bodies, treat as vertical: 2 km buffer	2
8. Anticlines: 2 km buffer	1
9. Volcanic units regardless of age: 5 km buffer	2
Geochemistry; anomalous direct and indirect pathfinder elements	
10. Stream sediment, direct: Au. (interpolated map—divided into five classes based on high to low concentration)	10, 8, 2, 1, 0
11. Stream sediment, key indirect: As, Sb, Hg, Te. (each element map was normalized (to provide equal influence) and then all elements were summed and the mean value was calculated—this map was divided into a five class map reflecting high to low concentration—class thresholds based on natural breaks in the data histogram)	6, 4, 2, 1, 0 by class
12. Stream sediment, possible indirect: Ag, Ba, Cs, Cu, Fe, Mo, Pb, Se, Si, Te, Tl, W, Zn. (each element map was normalized (to provide equal influence) and then all elements were summed and the mean value was calculated—this map was divided into a five class map reflecting high to low concentration—class thresholds based on natural breaks in the data histogram)	4, 3, 2, 1, 0 by class
13. Stream water, key indirect: As, Sb, Hg, Te. (each element map was normalized (to provide equal influence) and then all elements were summed and the mean value was calculated—this map was divided into a five class map reflecting high to low concentration—class thresholds based on natural breaks in the data histogram)	6, 4, 2, 1, 0 by class
14. Stream water, possible indirect: Ag, Ba, Cs, Cu, Fe, Mo, Pb, Se, Si, Te, Tl, W, Zn (each element map was normalized (to provide equal influence) and then all elements were summed and the mean value was calculated—this map was divided into a five class map reflecting high to low concentration—class thresholds based on natural breaks in the data histogram)	4, 3, 2, 1, 0 by class
15. Springs with CARLIN signature anomalous in Ag, Sb, As, Au, Ba, Hg, Ti, Tl. : Buffer 3km	2
16. Placer gold occurrences only where they fit Rasmussen's local derivation criteria: around Selwyn Plutonic Suite and within buffer of springs with Carlin signature. Buffer = 5 km	5
17. Lode mineral occurrences of the Carlin and other granite-related types (after Rasmussen, 2007; Cline and others, 2005; and NORMIN) were assigned to one of 2 categories: showing (weight 2), or anomaly (weight 1); 3 km buffer	2, 1
18. Airborne gamma ray spectrometry should detect potassic alteration zones that may be expressed as illite, dickite or potassium feldspar. (binary map of anomalous potassium concentration	1
19. Ph—sampled from water chemistry—data were interpolated and map divided into 8 classes reflecting acid to basic conditions	10, 9, 8, 7, 4, 3, 2, 0

TOTAL of 20 evidence maps used for producing the CARLIN potential map

The second hypothesis for Carlin deposits emphasizes the regional linear trends of the gold deposits that geologists have divided into regional ''trends'' (i.e. The Carlin trend, the Battle Mountain trend etc.). According to this hypothesis the plutons were not responsible for the heat, but were simply accessories. Instead, the extensional tectonic regime resulted in high heat flow that mobilized metal-bearing fluids to form the deposits. The fluids themselves were derived from meteoric water that penetrated the crust along deep-seated fracture systems created by the same extensional tectonism.

The metal contents of Carlin deposits, regardless of their hypothetical origins, tend to be distinctive with As, Sb, Hg, Ti and Ba accompanying Au and Ag. The suite of pathfinder elements is controlled by the geochemistry of the transporting fluids, especially at the cool temperatures at which these deposits tend to form.

The host rocks are primarily impure carbonate strata, typically argillaceous limestone and dolostone that were effective at channelling fluids while at the same time providing the reactive elements ($CaCO_3$) to alter the pH of the transporting fluids resulting in the precipitation of sulphide minerals.

Active fault systems are also thought to play a role in the formation of Carlin-Type deposits by localizing and concentrating deposits along fault traces with a reduction in ore thickness away from the fault zones. The faults act as fluid conduits transporting and concentrating fluids from large regions into focussed flow zones. Intersections of conjugate fault systems where permeability is the greatest are highly prospective zones.

Deformation structures such as anticlines may also play a significant role in the formation of Carlin-Type deposits. Although these structures may not have been active during the mineralization events, folding and modification of the sedimentary sequence in many cases resulted in an increase in permeability, especially in the dilational, anticlinal axis zones.

In the search for the Carlin-Type of deposit, the presence of other mineral deposits is often used as a vector, including linear strings of seemingly unrelated metal concentrations. Long-lived, deep-seated crustal sutures along which continents may have amalgamated are commonly the locus of a variety of metal-bearing fluids derived from intrusive and extrusive magma, regional metamorphic events and from the surface. As such deeply buried structures are rarely exposed and difficult to identify using geophysical techniques, they are often identified by the linear pattern formed by the deposits themselves.

More direct indicators of Carlin-Type deposits are fine-grained placer gold deposits with pathfinder elements that represent weathered and locally transported lode gold deposits. Placer-gold occurrences in many places have provided the first evidence of the presence of Carlin and other types of lode gold deposits.

The westernmost Nahanni River region has been identified as one of the most prospective in Canada for hosting Carlin-Type deposits (Rowan, 1989; Richards, 1989; Poulsen, 1996; Rasmussen and others, 2007). All of the elements identified as critical to the formation of a fine-grained disseminated sediment-hosted gold deposit (Carlin-Type) discussed above have been identified in the study area, except for the regional extensional tectonism.

APPLIED METHODOLOGY

Overview: Production of Mineral Potential Maps

Figure 4 provides a summary of the modelling process used to produce the various potential maps. For each deposit model, vectors (indicators) to mineralization were selected based on the exploration criteria discussed previously, in concert with

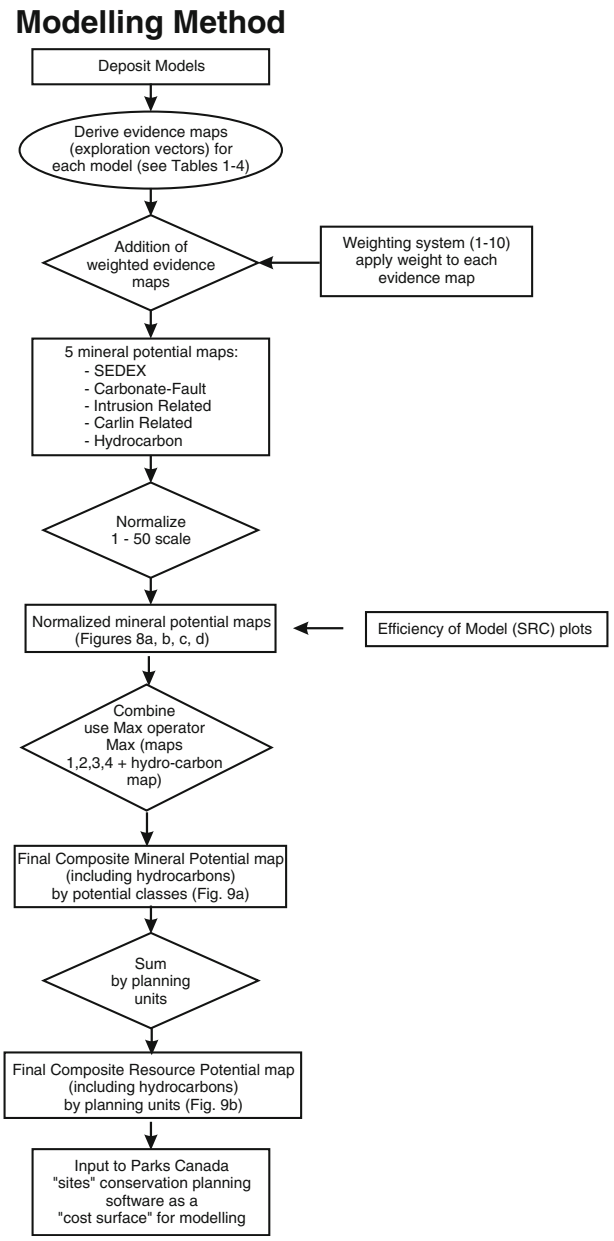

Figure 4. Flow chart for GIS modelling operations reported in this paper.

exploration knowledge of the area. Evidence maps (thematic data layers) were created based on these vectors and each map was weighted (Tables 1–4). The weights for each evidence map were subjective and are based on expert opinion (of the 3rd and 5th authors) in conjunction with regional exploration knowledge derived from literature searches and discussions with geologists from industry and provincial and territorial governments. It should be noted that weighted mineral occurrences for each style of mineralization were also used as evidence maps in the modelling process.

One primary potential map was produced for each of the four deposit models and one other for hydrocarbon potential. This was accomplished by combining the weighted evidence maps for each model, using a simple additive technique (weighted index-overlay) followed by normalization to a scale of 1–50 to ensure each of the four deposit maps had equal weight in the final, combined model. The hydrocarbon map was also normalized so that each of the three high-potential areas had a weight of 50 reflecting their high potential for hydrocarbons (K. Osadetz, pers comm., 2007). These four individual potential maps and the fifth hydrocarbon potential map (already converted into 1 class of very high potential) were then combined into one final mineral potential map using a MAX operator as outlined in Fig. 4. The rationale behind the MAX operator is that high potential for any one deposit model is sufficient on its own. If the additive function were to be used at this stage, this process would subdue a high-potential rating that is based on only one deposit model compared to a similar high potential rating that is derived for two or more deposit models. The final step was to partition the geologically based mineral potential map into drainage-defined planning units developed by Parks Canada for park planning purposes.

Plots showing the efficiency of the model (i.e. how well the potential map predicts the known occurrences; termed an SRC plot) for the final additive potential map were generated for each of the four deposit models to assess how well the map predicts the individual occurrences organized by deposit type. These graphs were produced by plotting cumulative area of each potential map (from highest to lowest potential) against the number of deposits predicted (Chung and Fabbri, 2003 and Harris and others, 2006a, 2006b).

Space does not permit showing the individual evidence maps for all four models. However to demonstrate the methodology, a complete set of evidence maps is shown in Fig. 5 for the SEDEX model only.

SEDEX Model

A total of 17 weighted evidence maps (Table 1; Fig. 5) were used to create an additive SEDEX mineral potential map (see Final Model section). The individual evidence maps are described below.

Favourable Rock Packages

Favourable rock packages included Cambrian to mid-Devonian transitional to deep basinal strata (Fig. 5a) which are established SEDEX hosts, as well as basinal Neoproterozoic Windermere Supergroup strata (shaly sandstone) (Fig. 5b). These strata may have been the source of metals to form the overlying SEDEX deposits as well as having potential to host SEDEX deposits in their own right. The former rock package is highly weighted (see Table 2), whereas the latter is assigned a lower weight due to its speculative genetic ties to the SEDEX model.

The early Silurian portion of the generally black, calcareous, graptolitic, Cambrian to Silurian shale in the Road River Group hosts the Howard's Pass deposits. These collectively represent one of the few giant to super giant SEDEX-type camps of the world. Of similar age but different in lithology, the carbonaceous cherty black shale of the Whittaker Formation also hosts similar stratabound zinc and lead sulphide minerals at Prairie Creek (one of the three types that constitute the fault-associated composite model). The total extent of the SEDEX portion of Prairie Creek is not known, but its presence supports the concept of a broader mineralizing event in the late Silurian. A second series of SEDEX-type mineral deposits, characterized by the Tom and Jason deposits in the Macmillan Pass area, is hosted by late Devonian to Mississippian siliceous black shale and conglomerate of the Earn Group. All of the Cambrian to Mississippian basinal strata together constitute the highly weighted first lithological evidence map.

East of the Earn Group tract, the contemporaneous grey silty shale units and the Besa River and Horn formations are not known to host mineral deposits. Neither formations display facies changes

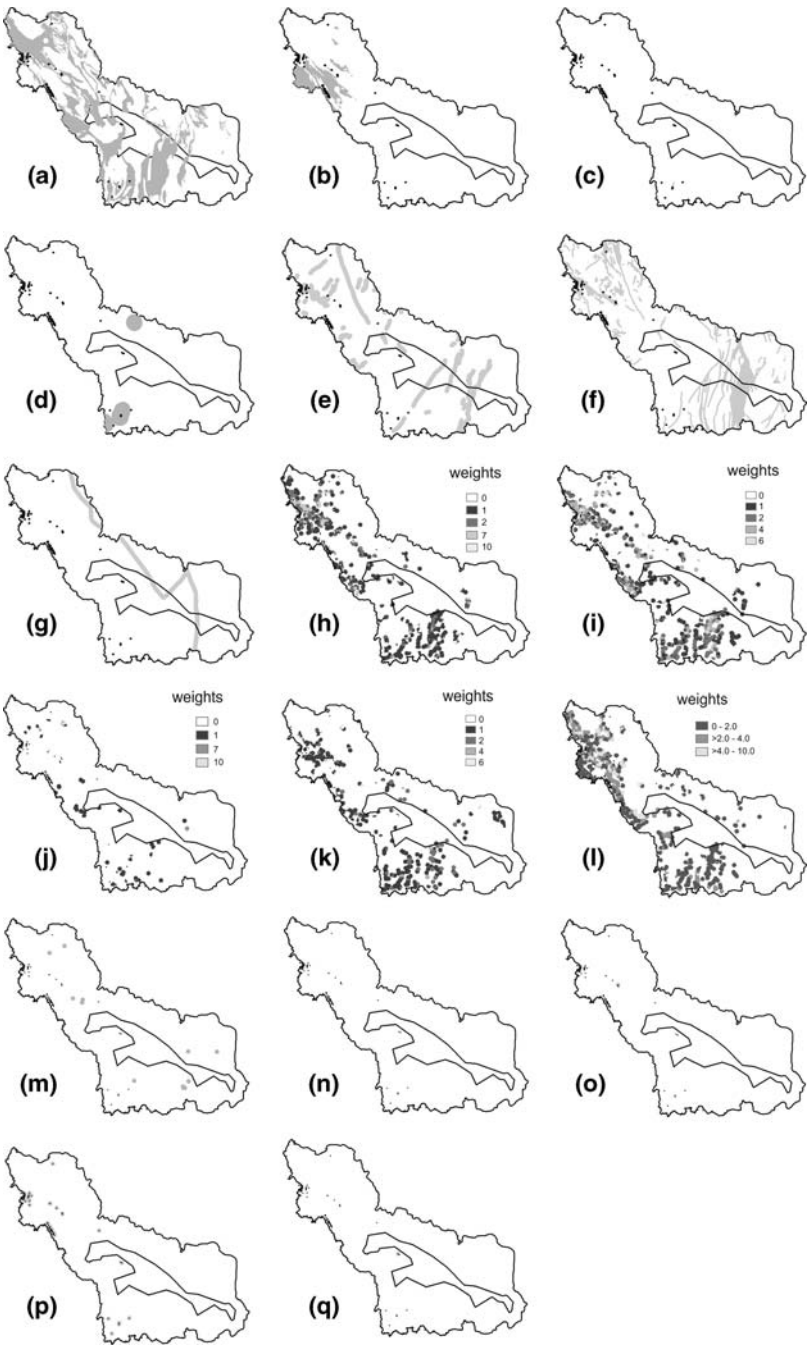

Figure 5. Evidence maps used for modelling SEDEX deposit type, (a) transitional to deep basinal strata, wt. = 10; (b) basinal Windermere strata, wt. = 3; (c) Cambrian to Ordovician volcanic units, wt. = 10; (d) 3 km buffer around volcanic units, wt. = 5; (e) 3 km buffer around growth faults, wt. = 2; (f) 2 km buffer around faults, wt. = 1; (g) carbonate-shelf facies change, 3 km buffer, wt. = 1; (h) stream sediment geochemistry, direct indicators; (i) stream sediment geochemistry, indirect (pathfinder) indicators; (j) stream water geochemistry, director indicators; (k) stream water geochemistry, indirect (pathfinder) indicators; (l) pH, water geochemistry; (m) 3 km buffer around anomalous springs, wt. = 2; (n) 3 km buffer around SEDEX occurrences, defined resources, wt. = 10; (o) 3 km buffer around SEDEX occurrences, wt. = 7; advanced prospects, wt. = 5; (p) 3 km buffer around SEDEX occurrences, showings, wt. = 2; and (q) 3 km buffer around SEDEX occurrences, anomalies, wt. = 1.

such as siliceous or highly carbonaceous zones, or conglomerate. Therefore these units are characterized as an unfavourable rock package and given no weight in this analysis.

Structural Features

Cambrian and Ordovician volcanic units (Fig. 5c), as well as proximity to these units (Fig. 5 d), are modelled in a similar fashion to faults, in that they represent deep crustal zones of weakness that may have channelled hydrothermal fluid flow. Growth faults (Fig. 5e) are interpreted as Laramide expressions of northeast-trending deep crustal offsets, the Leith Ridge and Fort Norman structures (Aitken and Pugh, 1984). These are interpreted as zones of weakness that caused subtle lateral facies changes and could have focussed the transport of hydrothermal fluids during sedimentation. They are now interpreted as reactivated in terms of steeply dipping cross faults that are discordant to northwesterly regional fold and thrust trends.

All other faults (excluding growth faults) (Fig. 5f) are mainly southwest dipping thrusts, some of which may have been primary depositional extensional faults that could have channelled mineralizing fluids but were reversed during the compressional Laramide deformation that formed the Selwyn and Mackenzie mountains.

A major carbonate-shale facies change (Fig. 5g) along the Ordovician to Devonian platform edge is interpreted as yet another favourable location for the development of structures that could have transported hydrothermal fluids.

Stream Sediment and Stream Water Geochemistry

Elements considered to reflect both direct and indirect evidence for SEDEX deposits (Table 1) were extracted from the stream sediment and water geochemical data sets (Fig. 3a). Variograms were constructed for each pathfinder element in order to determine a ''zone of influence'' around each sample point (see Harris and others, 2001). The zone of influence (typically 3 km) was used as a search radius for an inverse-distance-weighted (IDW) algorithm used to interpolate the data over selected favourable rock units. An advantage of this approach which utilizes a fixed radius is that areas characterized by a low density of sample points are not interpolated, thus reducing the introduction of artefacts and thereby increasing the certainty in the interpolation process. The interpolated map of each element was then normalized from either ppm or ppb to byte data (0–255) so that in the additive processes of combining the data all of the included elements would be equally weighted preventing any one element to dominate based on a wider data distribution range. A map showing mean normalized concentration was then produced by summing the normalized interpolated element maps and dividing by the number of elements. For example, the evidence map of direct SEDEX pathfinder elements obtained from stream sediment data was created by using the following formula:

$$(\mathrm{nAg} + \mathrm{nCu} + \mathrm{nPb} + \mathrm{nCu})/4$$

where n = normalized value.

This map was then broken into five classes based on natural breaks in the histograms of the normalized data. The classes were assigned subjective weights of 10, 7, 2, 1 and 0 for the highest to lowest mean concentrations, respectively. The entire data processing method (applied to the geochemical data for all deposit models) is summarized in Fig. 6.

This same process was repeated for the indirect SEDEX pathfinder elements: As, Ba, Cd, Cr, F, Mn, Mo, Ni, Sb and U. However the lower weights assigned to the five class normalized mean map (6, 4, 2, 1, 0) reflect the lower predictive power of the indirect pathfinder elements.

The same process was applied to the water geochemical data, excluding those pathfinder elements that were not determined (see Table 1). Figures 5h, i, j and k show the final five class normalized mean maps for the direct and indirect elements from the stream sediment and water geochemical data used to produce the SEDEX mineral potential map.

pH (Acidity of Stream Water)

The pH is lowered by the oxidation of sulphidic minerals under aqueous conditions to produce sulphuric acid. The pH in turn influences the transport of metals in water and their adsorption on to particulate matter in stream sediments. Low pH (acidic) water has enhanced capacity to transport most metals and may thereby enhance their geochemical expression. In neutral to alkaline environments the chemical mobility of many metals, including Zn, Ag

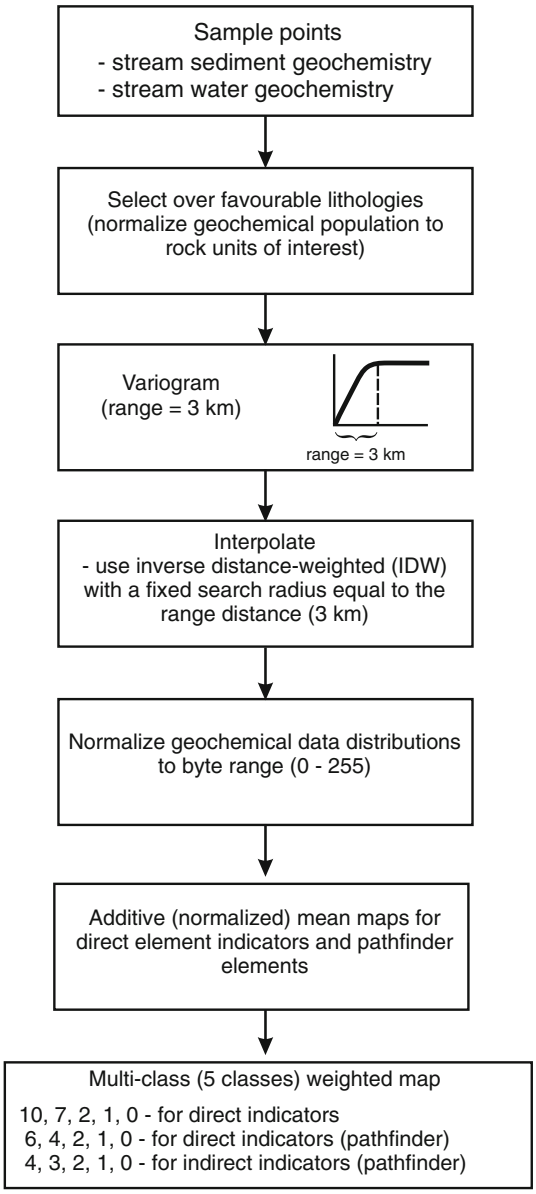

Figure 6. GIS modelling process to determine a ''zone of influence'' around sample points for interpolation of geochemical data between sites of stream sediment, stream water and spring water samples.

and Pb, and to a lesser extent As and Cd, is severely restricted (Plant and Raiswell, 1994). Conversely, metals such as U, Mo and V are relatively mobile. As the pH of stream waters exceeds 7.0 in much of the survey area because of the dominance of limestone, the geochemical dispersion of many elements is reduced in those areas. It is expected that pH will tend to be buffered consistently within rock units except for anomalous sites.

Using the above knowledge, an evidence map of pH was produced from the water geochemical data using the following method. The point data were interpolated using IDW with a 3 km fixed search radius as determined from a variogram (Fig. 6). This interpolated map was then divided into eight equal classes based on quartiles with the following weights (10, 9, 8, 7, 4, 3, 2, 0) representing extremely acidic to basic pH conditions, respectively (Fig. 5l). The more acidic conditions were given a higher weight to reflect more favourable environments assuming that the cause of the acidity was sulphide minerals such as sphalerite (zinc +/− silver), galena (lead +/− silver) and tetrahedrite (copper + silver), recognizing that pyrite and carbonaceous shale that contain no base metals also reduce pH.

Spring Water Geochemistry

Spring water sample sites were subjectively classified as favourable for SEDEX, based on anomalous pathfinder elements (all SEDEX anomalous springs from Table 5.12 of Hamilton and others (2003) and selected anomalous springs characterized as SEDEX from Table 6 of Caron, Grasby, and Ryan (2007)). The following pathfinder elements were considered as direct evidence: Ag, Cu, Pb, Zn; and as indirect evidence: As, Ba, Cd, Cr, Mn, Mo, Ni, pH, Sb, V. Those sites considered as anomalous for one or more elements indicating SEDEX were buffered to 3 km and assigned a weight of two (Fig. 5m).

Mineral Occurrences

Mineral occurrences of the SEDEX-type were assigned to one of four categories: defined resources (weight 10), advanced prospect (weight 7), showing (weight 4) and anomaly (weight 2). The weighted points were then buffered to 3 km representing a ''zone of influence'' (Fig. 5n, o, p, q). A distance of 3 km was chosen based on observations with respect to mineralization and alteration made in the field.

Carbonate-Fault Model

A total of 15 weighted evidence maps (Table 2) were used to create an additive Carbonate-Fault mineral potential map. This map indicates relative

potential for the presence of undiscovered zinc–lead–silver massive sulphide deposits that fit this composite model as described above in the deposit model overview section. The evidence maps are as follows.

Favourable Rock Units

Favourable host rocks include dolostone of the Devonian to Cretaceous Manetoe, Presqu'ile and Grizzly Bear formations (diagenetic facies) (weight 10), middle Devonian strata (weight 5), Cambrian to early Devonian carbonate platform strata (limestone, dolostone) (weight 5), Cambrian to early Devonian calcareous shale (weight 2) and proximity to the diagenetic facies listed above (3 km buffer, weight 5).

The Manetoe and Presqu'ile facies are diagenetic and/or hydrothermal alteration products of carbonate lithofacies (limestone and dolostone) that constitute the Mackenzie Platform (Morrow, Cumming, and Aulstead, 1990). This style of alteration is associated with reef-related dolomite diagenesis and with the passage of hydrothermal fluids, an alteration style that is present in and around significant carbonate-hosted base-metal deposits in western Canada (i.e. Pine Point, Robb Lake and near Prairie Creek (Paradis, 2007)).

Structural Features

Growth faults (3 km buffer, weight 2), all other faults (2 km buffer, weight 1) and the trend of the facies change between the Devonian carbonate and shale assemblages, as per the SEDEX model (2 km buffer, weight 1) were used as evidence maps for the presence of undiscovered Carbonate-Fault-related deposits. As for the SEDEX deposit model, these features were likely to have focussed the flow of hydrothermal fluids.

Stream Sediment and Stream Water Geochemistry

Four evidence maps were created based on direct and indirect elements for Carbonate-Fault-related mineralization from the stream sediment and stream water geochemical data. The processing and weighting strategy was the same as described for the SEDEX model, however, different suites of pathfinder elements were used as listed in Table 2.

Spring Water Geochemistry

Spring water sample sites were subjectively classified as favourable for Carbonate-Fault deposits based on anomalous pathfinder elements (Prairie Creek mine water from Table 5.12 of Hamilton and others (2003) and selected anomalous springs from Table 6 of Caron, Grasby, and Ryan (2007)). The following pathfinder elements were considered: direct (Ag, Cu, Pb, Zn) and indirect (Cd and Sb). Those considered anomalous for one or more of these elements were assigned a weight of 2 with a 3 km buffer.

Mineral Occurrences

Mineral occurrences classified in the Carbonate-Fault model were assigned to one of two categories: defined resources (weight 10) and showing (weight 4). These classified points were buffered to 3 km representing a potential ''zone of influence'' reflecting the same distance rationale as discussed above for the SEDEX model.

Intrusion-Related Model

A total of 14 weighted evidence maps (Table 3) were used to create an additive Intrusion-Related mineral potential map. These are described below.

Favourable Rock Units

Each intrusion (pluton) was assigned to one of three groups based on qualitative geological assessment of their potential (high, medium, or low) to host or be spatially associated with undiscovered Intrusion-Related deposits, following the classification of Rasmussen and others (2007). Additional geological knowledge provided by Barnes, Groat, and Falck (2007) and Yuvan, Shelton, and Falck (2007) was also considered. For modelling purposes, any mapped hornfels associated with the margin of a pluton was included as part of that pluton, based on the assumption that hornfels (contact metamorphosed sedimentary rock) was caused by a shallowly underlying portion of a pluton below the hornfels. The plutons were buffered at three different distance intervals and within each pluton itself reflecting zones of different alteration intensity as

observed from various field studies and mapping initiatives. The proximal zone (1 km buffer outside and inside each pluton representing a zone of maximum alteration) was assigned the highest weight.

Shaly limestone units situated within 20 km of any pluton were also weighted for their potential to host undiscovered skarn deposits (Fig. 7). Units thought to have the highest potential for skarn deposits are defined by their content of impure limestone. The highest rank of 10 was assigned to the heterogeneous limestone-bearing units (Vampire and Sekwi formations) that include the immediate host of the Cantung Mine.

Structural Features

A fault density map was produced from a vector file of faults using a line density algorithm in the GIS. The basic premise is that faults acted as conduits for mineralizing fluids either from the plutons themselves or remobilized from the host rocks as a result of pluton emplacement. This algorithm produces a density map based on the number of faults within a 5 by 5 km neighbourhood. This map was divided into three classes based on natural breaks in the data histogram; high, medium and low density; and assigned weights of 5, 3 and 1, respectively.

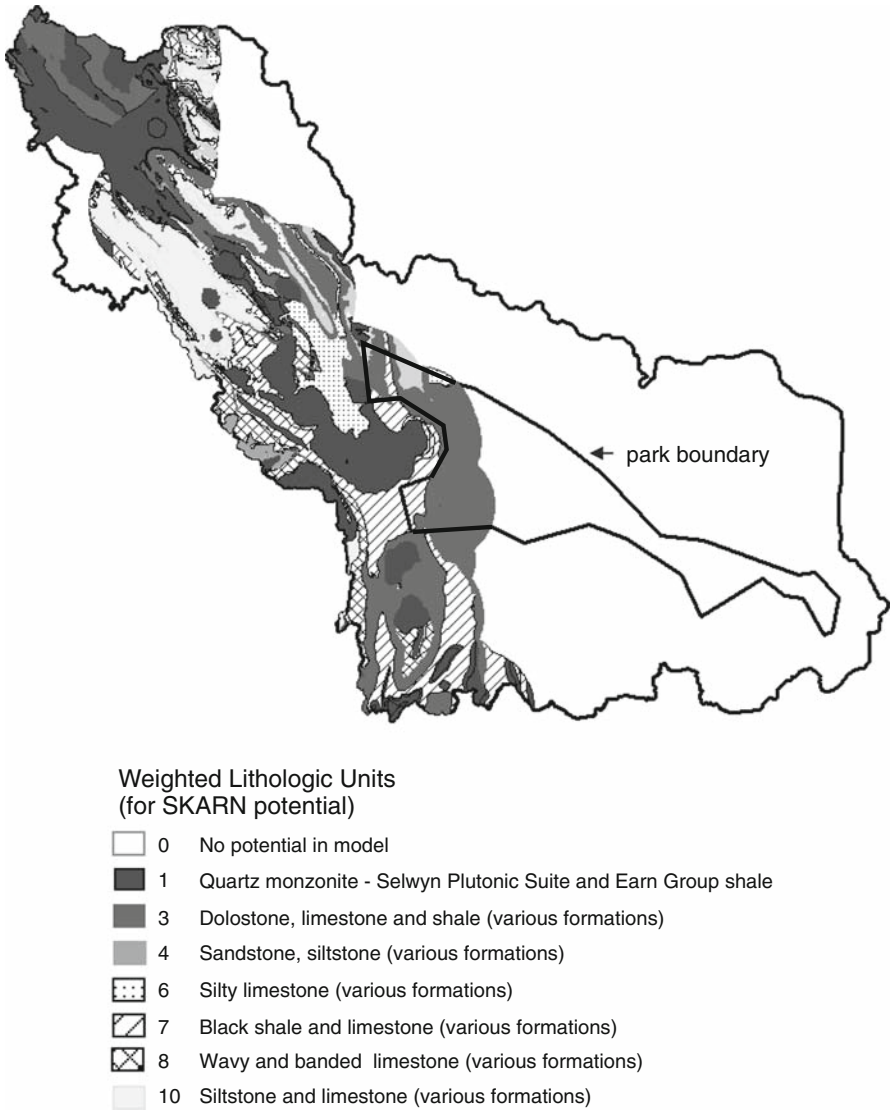

Figure 7. Rated geology within areas of influence of intrusions in Selwyn Plutonic Suite, used for modelling Intrusion-Related and Carlin-Type gold deposit potentials. Dark shades are assigned to low potential, light shades to high.

Stream Sediment and Stream Water Geochemistry

Two multi-class additive and normalized maps were produced showing direct and indirect pathfinder elements from the stream sediment data. Two maps were similarly produced from the water geochemical data. The same geochemical processing method described for the SEDEX model (Fig. 6), using a different suite elements for direct and indirect evidence (see Table 3), was adopted for the Intrusion-Related model.

Spring Water Geochemistry

Spring-water sample sites were subjectively classified as favourable for Intrusion-Related mineralization based on anomalous pathfinder elements (three examples labelled 'tungsten skarn' from Table 5.12 of Hamilton and others (2003) and selected anomalous springs from Table 6 of Caron, Grasby, and Ryan (2007)). Direct pathfinder elements include W, Cu, Pb, Zn; and indirect pathfinder elements include Ag, As, Au, Bi, F, Sb, Sn and Te. As for the SEDEX model a 3 km buffer (zone of influence) around each anomalous sample point was produced and a weight of 2 was assigned for this evidence map.

Mineral Occurrences

Mineral occurrences of the Intrusion-Related model (after NORMIN, Barnes, Groat, and Falck, 2007; Rasmussen and others, 2007, and Yuvan, Shelton, and Falck, 2007) were assigned to one of four categories: defined resources (weight 10), advanced prospect (weight 5), showing (weight 2), and anomaly (weight 1). As for the SEDEX model, each weighted occurrence was buffered to a distance of 3 km representing a ''zone of influence'', again using the distance rational discussed for the SEDEX model.

Carlin Model

A total of 20 weighted evidence maps (Table 4) were used to create an additive mineral potential map for undiscovered Carlin-Type lode gold and/or related placer deposits. The evidence maps are described below.

Favourable Rock Units

Many researchers feel that Carlin-Type mineral deposits share a strong association with late Cretaceous plutons (e.g. Poulsen, 1996; Rasmussen and others, 2006; 2007). In the Nevada Carlin-type locality, carbonate units are essential as host rocks. Thus, the same three pluton groups and variegated limestone units, with the same buffering and weighting strategies as the Intrusion-Related model, were applied to the Carlin-Type model.

Structural Features

With the initiation of fluid systems, transportation corridors were also needed to focus fluid flow. Additional dilational zones such as anticline axes may have enhanced permeability and therefore are also an important structural feature to model. Thus, as with the Intrusion-Related model, growth faults within 20 km of a granite body were buffered to 2 km reflecting a zone of influence and assigned a weight of 1. All other faults were buffered to a distance of 2 km but only on the down-dip side (i.e. toward the southwest) and weighted as 1. Fault intersections were buffered to 2 km with a weight of 2 and within 20 km of a granite body. Anticlinal axes were buffered to 2 km with a weight of 1. A 5 km buffer (weight 2) was assigned to all volcanic units and the units themselves were weighted 2. Regardless of the age of extrusion, volcanic units are modelled as indicating deep-seated basement structures. All of the above structural evidence maps highlight features that may have served as conduits for mineralizing fluids. Rational for buffer distances were based on field observations and exploration knowledge.

Stream Sediment and Stream Water Geochemistry

Three evidence maps were created from the stream sediment data; one based on direct pathfinder elements, one on indirect pathfinder elements and one on possible pathfinder elements (see Table 4). The same processing and weighting strategy described for the SEDEX model was also used for the Carlin model. The only exception was the addition of a possible pathfinder map whose five normalized classes are assigned weights of 4, 3, 2, 1 and 0. This map was lesser ranked due its lower

predictive power. The only stream sediment element used for direct evidence was Au.

The same procedure was repeated for the stream water geochemical data using a modified suite of elements (Table 4). Only two evidence maps, indirect pathfinders and possible pathfinders, were produced from the water geochemical dataset, because no direct evidence (Au) was analyzed.

pH

The same strategy and weights used to create pH evidence maps for the SEDEX and Intrusion-Related models were applied to the Carlin modelling.

Spring Water Geochemistry

Springs with a ''Carlin signature'' in anomalous pathfinder elements (Ag, Sb, As, Au, Ba, Hg, Ti, Tl) were buffered to a distance of 3 km and assigned a weight of 2.

Placer Gold Occurrences

Placer gold occurrences are historically the first direct indicator in the discovery history of many Carlin-Type deposits and these were selected from the mineral deposits database (NORMIN). Given the importance of intrusions to the composite Carlin model used in this analysis, placer gold occurrences were included in the model only where they fit local derivation criteria within the buffer of a pluton or a spring with plutonic characteristics. Thus not all of the eastern Nahanni gold occurrences were included. A 5 km buffer around each placer gold occurrence with a weight of five was employed to create the evidence map.

Lode Gold Occurrences

Lode gold occurrences that are compatible with the Carlin model (after Rasmussen, 2007; Cline and others, 2005; and NORMIN) were assigned to one of two categories; showing (weight 2), or anomaly (weight 1) and each group of points was buffered to 3 km creating two evidence maps.

Composite Model

The four additive-normalized potential maps are shown in Fig. 8 a, b, c, d (see Fig. 4 and previous discussion for method). These four maps and the single class hydrocarbon potential map of Osadetz, Chen, and Morrow (2003) were used to create the composite potential map using the following equation:

$$\mathrm{MAX}(\mathrm{Carlin, Fault, Intrusion, SEDEX, Hydrocarbon})$$

– where the input maps represent the four additive and normalized potential maps and the hydrocarbon map.

This composite potential map (Fig. 9a) which was divided into five discrete classes was used as the basis for selecting conservation areas as it formed the ''cost layer'' that was used in the site selection process undertaken by Parks Canada. Fig. 9b shows a map of Parks Canada's planning units in which the maximum value (based on Fig. 9a) for each planning unit was calculated by using a zonal analysis in the GIS.

The rational for using a MAX operator was to ensure that a planning unit was labelled high potential (thus a high cost) even if only one of the four potential maps showed the area to be of high potential. Thus the planning units shown in light grey on Fig. 9b represent areas where one or more of the five potential maps indicate high mineral or energy resource potential. This strategy provides a comprehensive estimate of mineral potential.

RESULTS

Validation

Plots showing how well each mineral potential map predicts the known occurrences (known as efficiency of classification or SRC plots) were generated (Fig. 10a–d) for the purpose of validating the models. These plots show the number of occurrences predicted as a function of area, ranked from high to low potential, on each of the additive—normalized mineral potential maps for each deposit type (Fig. 8). Considering the top 5% of the highest potential areas, the SEDEX model is the best predictor with approximately 80% of the SEDEX-style

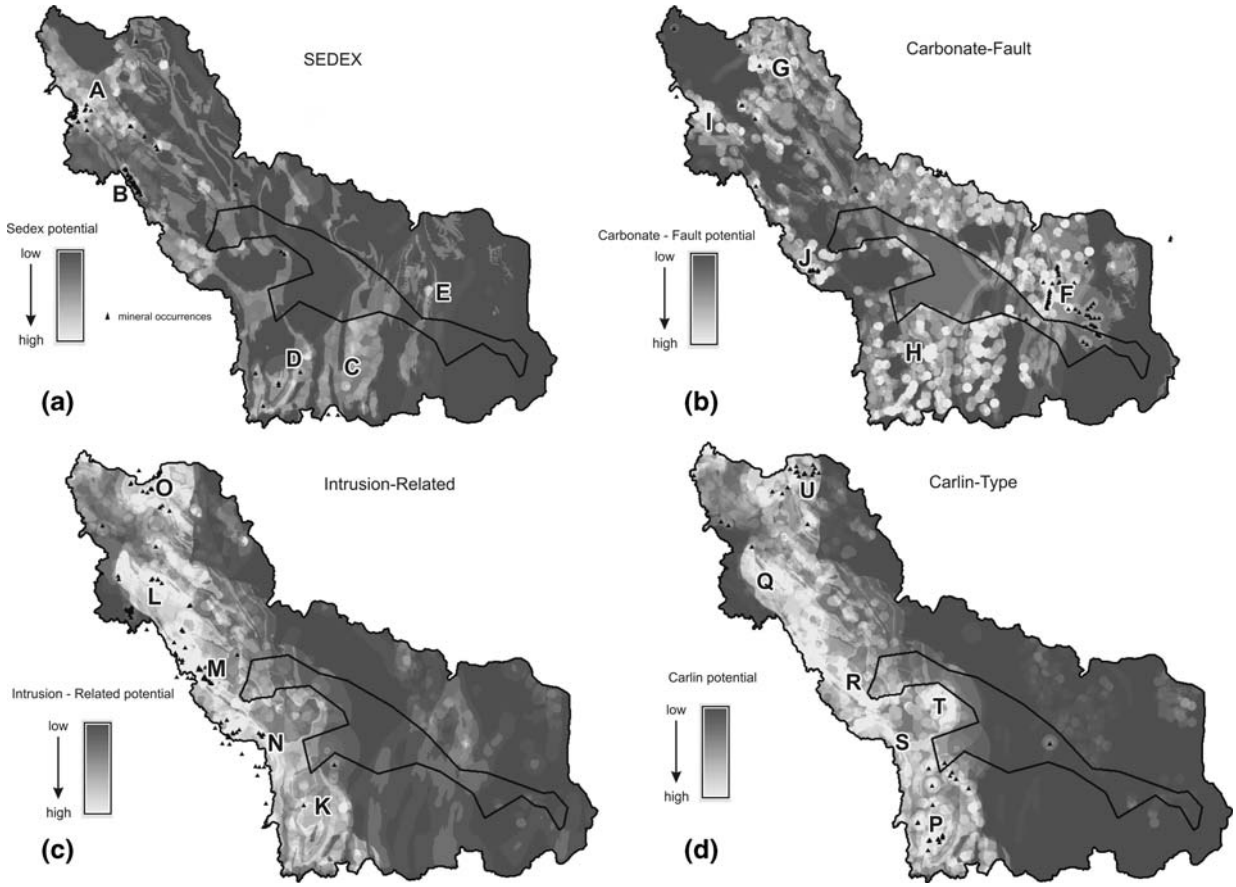

Figure 8. Final mineral potential maps for four mineral deposit models. Locations of mineral occurrences assigned to each of deposit models are shown for reference. Additive—normalized mineral potential maps used to create final potential map are shown in (a) SEDEX, (b) Carbonate- Fault, (c) Intrusion (Pluton) related, (d) Carlin-Type. Areas of highest potential are indicated by UNIQUE CAPITAL LETTERS and explained in text.

mineral occurrences being predicted. The Intrusion-Related (Pluton) model is next best, predicting about 60%, the Carlin-Type model slightly weaker at 40%, and the Carbonate-Fault model is the least predictive, with only 30% success. Considering the top 1% of the high potential area, the SEDEX model is again the best, predicting close to 50% of the SEDEX occurrences. The Intrusion-Related and Carbonate-Fault models predict 20% of its style of mineral occurrences, whereas the Carlin-Type model that predicts only 11%. Each of the individual models is at best only moderately predictive, although all four models predict 100% of the associated mineral occurrences in approximately 30% of the high potential area. The consistently poorer performance of the Carlin-Type potential map suggests that the deposit model is not particularly characteristic of these types of mineral occurrences at least within the study area.

Geological Interpretation

This section relates the areas of highest mineral potential as established by GIS analysis and modelling, in qualitative terms, to mineral deposit models and the geological and geochemical evidence supporting them. In a number of places there is overlap between the evidence for different deposit models and their quantitative GIS model results. Geographic and mineral potential areas of interest referred to below are represented in Fig. 8.

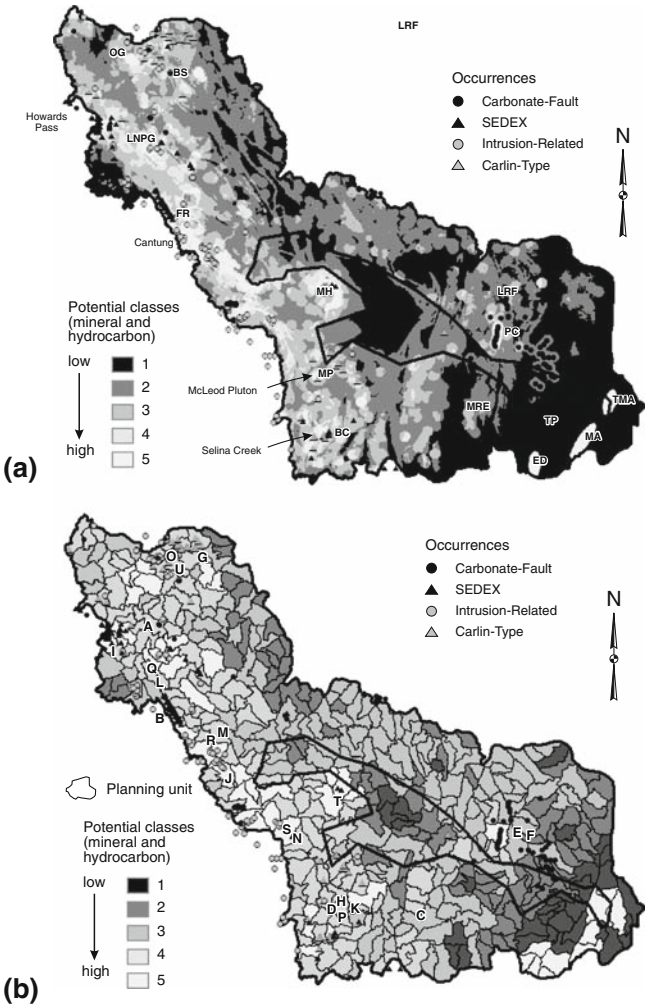

Figure 9. Composite mineral potential maps. Mineral occurrences by type are shown for reference. (a) Final mineral potential map generated by combining maximum values of individual additive—normalized potential maps for each deposit model as well as potential map for Hyrdocarbons, (b) Resource potential apportioned to park planning units using MAX operator. See text for explanation.

SEDEX Zinc–lead–silver

Five areas of interest on the final SEDEX potential map (Fig. 8a) are discussed next.

Area A in the northwest section of the study area contains some of the Howard's Pass deposits. The high potential area containing these deposits highlights the northwest part of a southeast-northwest- trending linear zone within the study area, informally known as the ''zinc corridor'', extending from the northwest end of the existing park reserve and the Flat River Valley to the Howard's Pass deposits. A separate sub-parallel strand of this corridor contains a high potential zone (area B) northwest of the Cantung deposit.

Area C represents a broad area of relatively high potential in the Meilleur River Embayment of the Selwyn Basin, hosted by the Road River Group, but partially masked by the younger Besa River Formation. This area is generally under-explored due to its remoteness but was previously highlighted by the Nahanni MERA 1, along the western edge of the Tlogotsho Plateau. The Meilleur River Embayment had earlier been identified as an important eastern extension of the Selwyn Basin by Morrow and Cook (1987). Despite the lack of exploration

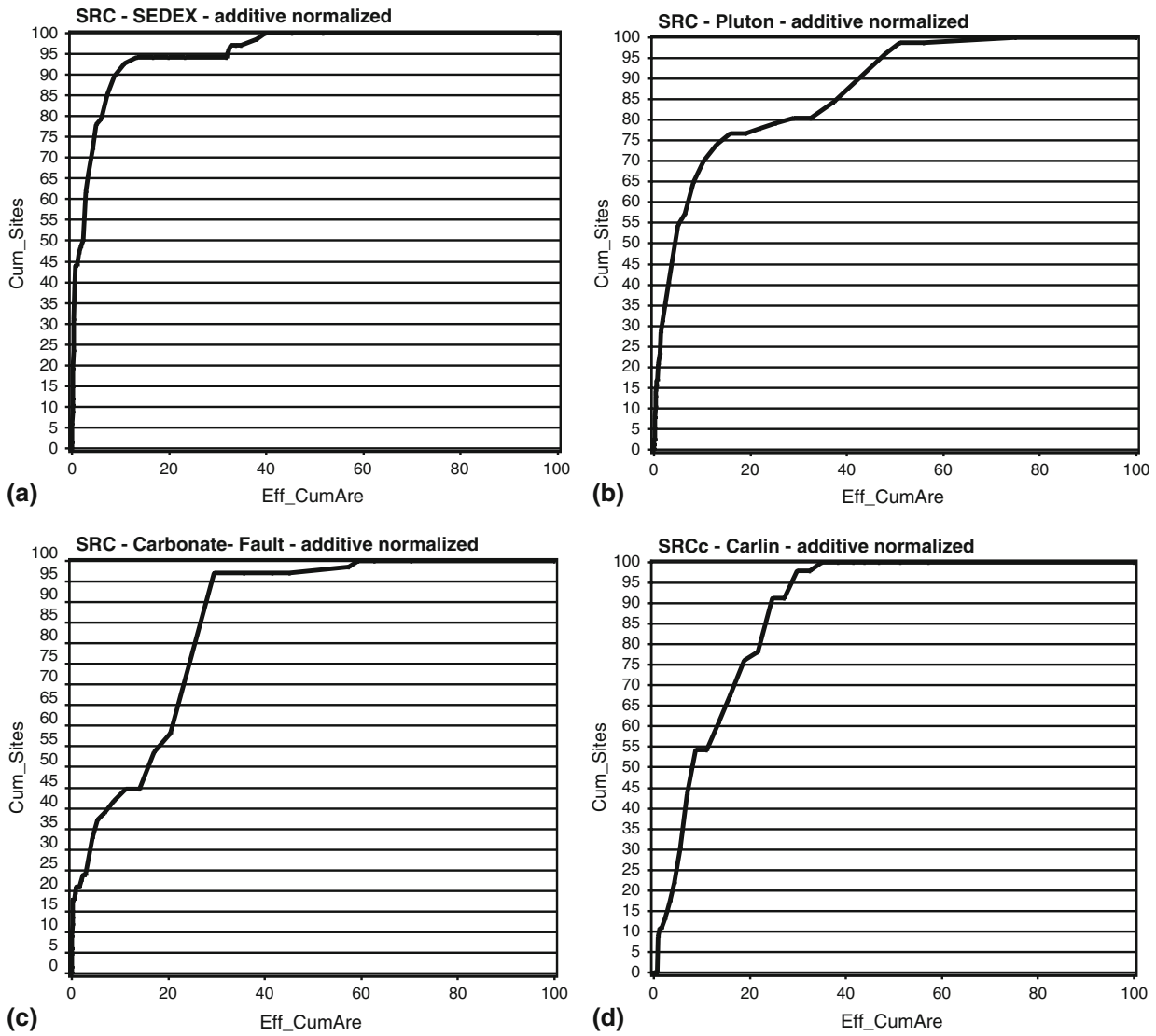

Figure 10. Efficiency of classification (model) graphs (SRC) for each of four deposit models in this GIS study, showing how well potential maps predict individual occurrences classified by deposit type. (a) Sedex additive- normalized (b) Plutonic additive – normalized (c) Carbonate- Fault—additive—normalized (d) Carlin additive –normalized. These plots show number of occurrences predicted as a function of area, ranked from high to low potential, on each of additive—normalized mineral potential maps for each deposit type. *Cum_Sites* represents number of occurrences (% of total) along *Y* axis and *Eff_CumAre* represents cumulative area of each potential map along *X* axis.

interest, this MERA 2 study has quantitatively reinforced evidence that the Meilleur River Embayment has relatively high potential for the presence of undiscovered SEDEX deposits based on the additive favourability of stream sediment, stream water and spring water geochemistry, northeasterly growth faults associated with the Leith Ridge basement structure, and favourable rock units throughout the area.

Area D in the vicinity of the Selena Creek deposit represents an area of relatively high potential, very much like that of Area C and underlain by the Road River Group within the Selwyn Basin proper. This area is characterized by rolling vegetated hills with little exposure except where dissected by deep canyons. Some zinc showings have been identified by the limited exploration efforts in this area. The regional northeasterly trend of high mineral potential

from the Prairie Creek to Meilleur River areas continues toward the southwest into this area, parallel to the deep-seated Leith Ridge structure.

Area E represents the northeastern extension of the Leith Ridge trend established by areas C and D, into the MacDonald Platform. This area is enhanced in potential by the growth fault attribute contributed by the carbonate-shale facies change that trends northerly along the Prairie Creek subembayment of the Meilleur River Embayment. Stream sediment, stream water and spring water geochemical data further support this designation.

Carbonate-Fault

Figure 8b shows mineral potential maps for the Carbonate-Fault zinc–lead–silver deposit model. A large area around the Prairie Creek deposit (Area F) containing many fault-related prospects has been classified as high potential based on this model. This rating is supported by favourable stream sediment chemistry, a high density of mapped faults and the presence of diagenetically altered limestone and dolostone units (Manetoe facies).

The Broken Skull area (Area G) is in the vicinity of the Broken Skull Fault, which is interpreted as a reactivated growth fault due to lithological changes across it. A number of anomalous hot springs in this area, with geochemistry suggestive of mantle fluids, support the inference that this fault is long-lived and deep-seated. This area is also characterized by anomalous stream sediment geochemistry.

Area H in the vicinity of the Selena Creek deposit is classified as higher in potential due to anomalous sediment geochemistry, favourable rock units and the presence of a number of north-trending faults. Some SEDEX prospects have been identified in this area as well as the high potential for Intrusion-Related mineralization may reflect an overlap in the genetic deposit models. The plutons in this vicinity may have acted as heat sources for re-mobilizing mineralized fluids along major faults.

Areas I (Howard's Pass) and J (southeast of Cantung) are located along the western strand of the ''zinc corridor'', delineated here primarily by anomalous stream sediment geochemistry, favourable basinal shale packages and a high density of faults.

A southeast-northwest trending divide is apparent between the high potential zones F and G in strata of the Mackenzie Platform, and areas H, I and J within the Selwyn Basin, that may reflect an overlap of Intrusion-Related models with SEDEX parameters. There are some examples of Carbonate-Fault occurrences in the southwestern area, but most of these show evidence of higher temperatures, favouring classification as Intrusion-Related instead.

Intrusion-Related

Figure 8c shows the Intrusion-Related mineral potential map. Obvious high-potential areas are restricted to the western portion of the region in proximity to the plutons. Area K around and to the north of Selena Creek is modelled as high in potential by virtue of its proximity to the ''McLeod and Big Charlie plutons'', intersecting carbonate units, anomalous geochemistry (particularly stream sediment), anomalies in spring waters and anomalous geophysical signatures. This area also contains a number of skarn occurrences.

Area L-M-N is a broad zone of high potential related directly to the Tay River plutonic suite. Its favourability is supported in part by anomalous stream sediment geochemistry, as well as carbonate units within the pluton buffers.

Area O is centred near O'Grady Lakes/Moose Ponds, covering the O'Grady batholith of the Tombstone plutonic suite and a number of high-ranking Intrusion-Related mineral prospects. In addition to anomalous stream sediment geochemistry, the pluton-buffered areas also contain favourable carbonate units and several Intrusion-Related anomalies represented by pathfinder elements in spring waters.

Carlin-Type

Figure 8d shows the Carlin-type Au potential map. An expansive area of high potential occurs in the vicinity of the Selena Creek placer deposit (Area P). This area has been classified as high potential based on a series of placer gold showings, favourable pathfinder elements (As, Sb, Hg, Ti and Ba accompanying Au and Ag), lithology, proximity to plutons and position at the southern end of a regional trend of existing gold prospects and deposits extending to Alaska.

The linear ''zinc corridor'' (Area Q-R-S) which contains both the Howard's Pass and the Cantung

regions is divided and partly overlapped by the high potential area for Carlin gold-type mineralization based on the proximity to plutons, a high density of anticlines and along a trend of numerous showings to deposits including one active mine. This area illustrates an overlap in parameters with the Intrusion-related model.

The high potential rating of Area T is a result of the intersection of the Mount Hamilton pluton buffer with favourable carbonate lithology, anomalous geochemical data from stream sediment, stream water and springs, as well as minor placer gold occurrences.

Area U, around and to the east of the O'Grady batholith, is similar to Area T with the added influence of favourable structural parameters such as faults parallel to the Broken Skull River.

DISCUSSION AND SUMMARY

Figures 9a, b present the composite mineral (and hydrocarbon) potential based on all of the models discussed above. Twelve per cent of the park expansion study area is characterized by moderate to high non-renewable resource potential, with restricted areas of very high potential. The high potential ratings are consistent with previously published, aerially or topically restricted resource assessments by Jefferson and Spirito (2003) and Lariviere and others (2006). Although still not all-encompassing, this GIS analysis achieves more comprehensive and objective results than the previous assessments by:

- incorporating broader and more advanced sampling and analytical techniques for the field and laboratory geochemistry,
- enhancing regional geological and geophysical knowledge,
- inclusion of quantitative spatial modelling in a GIS that has applied state-of-the-art integration methods to combine a knowledge-driven weighted dataset of deposit models, with the geochemical and geological data.

However, the mineral potential maps are constrained by:

- the present knowledge base
- the use of only four enhanced composite deposit models that together with the hydrocarbon map represent all non-renewable resource types known or thought to be important in the Nahanni Park area
- a limited number of evidence maps used to produce each map
- a subjective knowledge-driven weighting system for evidence layers.

This entire resource assessment process is knowledge-driven and the maps generated represent "our best estimate" of relative mineral potential given the limitations discussed above. However during our experiments to generate data-driven weightings we found that the knowledge-driven estimates are reasonable although adjustment of the weights and inclusion of other evidence may improve the performance of each map as the predictive power of the maps were moderate at best (Fig. 10). These maps would likely change in various areas with increased exploration knowledge, the availability of more (uniformly distributed) geoscience data for additional evidence maps, and further data-driven modelling to refine the weighting systems.

There is much evidence to indicate that where there is sufficient number of mineral occurrences, data-driven methods typically out-perform knowledge-driven techniques (Harris and others, 2001). Subjectivity and uncertainty were introduced in the initial definition of at least two of the deposit models: Intrusion-Related and Carbonate-Fault, each of which is a composite of at least three individual deposit types. It is likely that if each individual deposit type was modelled separately, the results may have been more discriminating. Subjectivity was required to select the various evidence maps for each of the models, as well as the applied weighting system. This added uncertainty to the modelling process which in turn may have resulted in less predictive maps. Furthermore the assignment of each mineral occurrence to one of the four deposit models introduced subjectivity.

In this article the mineral occurrences were used in the modelling process to help establish potential for each deposit type although in a different manner than used in typical data-driven modelling processes where the weighting system is defined by the number of occurrences falling on the favourable areas of each evidence map. If more occurrences fall on the favourable areas than would be expected to occur by chance then the evidence map would receive a high weight in the modelling process. In this article as stated previously a

knowledge-based approach was used to define the weights. However, the mineral deposit data divided into classes of importance and weighted accordingly were used directly as evidence maps in the modelling process. Recent work by Harris (in press) indicates that this approach in which the deposits are used as evidence maps performs as well as traditional data-driven approaches in which the location of the deposits are used to drive the modelling process.

Several areas within the study area were identified as having very high mineral potential. For SEDEX zinc–lead–silver type deposits, five areas were identified: (A) Howards Pass at the northwest end of the 'zinc corridor'; (B) another strand of this corridor northwest of Cantung; (C) the Meilleur River Embayment; (D) Selena Creek; and (E) east of Prairie Creek. For carbonate fault zinc–lead–silver deposits, five areas are highlighted: (F) Prairie Creek; (G) Broken Skull Fault; (H) Selena Creek; (I) Howard's Pass; and (J) southeast of Cantung. For intrusion-related deposits, three areas stand out: (K) Selena Creek; (L, M, N) a broad zone intruded by the Tay River plutonic suite including Cantung; and the (O) O'Grady batholith. Finally, for the Carlin-type lode and/or placer gold deposits, six areas have high ratings: (P) Selena Creek; (Q, R, S) a broad linear zone of intrusions dividing and overlapping the 'zinc corridor'; (T) surrounding the Mount Hamilton pluton; and (U) in and around the O'Grady batholith. High natural gas potential was assessed under MERA 1 p in the southeast corner of the study area, over the untested Etanda Dome and Twisted Mountain Anticline, as well as over the partially explored Mattson Anticline.

The use of GIS analysis procedures has greatly facilitated the process of producing mineral potential maps and transferring the results to Parks Canada as part of the MERA process. This method is an improvement over the traditional ''light table'' approach of overlaying maps and making visual assessments of mineral potential that have been historically used for MERA. The strictly GIS-based cost-benefit analysis utilizing these results partitioned into park planning units should not however replace round-table discussion and deliberation. Economic and strategic analysis will help the stakeholders understand the relative values of the various park attributes and cost factors, such as non-renewable resources with the aid of these GIS results.

ACKNOWLEDGMENTS

This article builds on all of the contributions made by the Nahanni MERA 2 participants, as acknowledged by the citations of their 2007 papers in this volume. Parks Canada provided substantial funding of this study through the MERA Process, with interdepartmental guidance from Indian and Northern Affairs Canada, Government of the Northwest Territories, Natural Resources Canada and Environment Canada. Programme leadership within Natural Resources Canada was provided by Margo Burgess, Manager of the Legislated Environmental and Resource Assessment Program of Earth Sciences Sector. Interaction with David Murray and Phil Wilson of Parks Canada facilitated GIS partitioning of results into the planning units. Critical reviews by Mark Mihalasky, Vesa Nykanen, Eric Grunsky, Tracy Lynds and Barham Daneshfar are much appreciated and have led to a much clearer presentation of this work. Editing by Elizabeth Ambrose and drafting assistance by Sue Davis are gratefully acknowledged. This is Geological Survey of Canada (GSC) contribution # 20070576.

REFERENCES

Aitken, J. D., and Pugh, D. C., 1984, The Fort Norman and Leith Ridge structures: major, buried, Precambrian features underlying Franklin Mountains and Great Bear and Mackenzie plains: B Can. Petrol. Geol., v. 32, p. 139–146.

Barnes, E. M., Groat, L. A., and Falck, H., 2007, A review of the late Cretaceous Little Nahanni Pegmatite Group and associated rare-element mineralization in the Selwyn Basin area, Northwest Territories, *in* Wright, D. F., Lemkow, D., and Harris, J. R. eds., Mineral and Energy Resource Assessment of the Greater Nahanni Ecosystem Under Consideration for the Expansion of the Nahanni National Park Reserve, Northwest Territories: Geological Survey of Canada, Open File 5344, p. 191–202.

Bonham-Carter, G. F., 1994, Geographic information systems for geoscientists: modelling with GIS: Pergamon, Oxford, 398 p.

Carne, R. C., and Cathro, R. J., 1982, Sedimentary exhalative (SEDEX) zinc-lead-silver deposits, northern Canadian Cordillera: Can. Inst. Min. Metall. Bull., v. 75, p. 66–78.

Caron, M.-E., Grasby, S. E., and Ryan, M. C., 2007, Spring geochemistry: a tool for exploration in the South Nahanni River basin of the Mackenzie Mountains, Northwest Territories, *in* Falck, H., Wright, D. F., and Harris, J., eds., Mineral and Energy Resource Potential of the Proposed Expansion to the Nahanni National Park Reserve, North Cordillera, Northwest Territories: Geological Survey of Canada, Open File 5344, p. 31–73.

Carson, J. M., Dumont, R., Potvin, J., Buckle, J., Shives, R. B. K., and Harvey, B., 2007a, Geophysical Series—NTS 95F—Virginia Falls, Northwest Territories: Geological Survey of Canada, Open File 5154, 1 CD-ROM.

Carson, J. M., Dumont, R., Potvin, J., Buckle, J., Shives, R. B. K., and Harvey, B., 2007b, Geophysical Series—NTS 95D and 95E—Flat River, Northwest Territories: Geological Survey of Canada, Open File 5160, 1 CD-ROM.

Carson, J. M., Dumont, R., Potvin, J., Buckle, J., Shives, R. B. K., and Harvey, B., 2007c, Geophysical Series—NTS 105H and 105I—Little Nahanni River, Northwest Territories: Geological Survey of Canada, Open File 5164, 1 CD-ROM.

Charbonneau, B. W., 2007, Evaluation of airborne radiometric and magnetic data in the vicinity of the Nahanni National Park Reserve, Northwest Territories, Canada, *in* Wright, D. F., Lemkow, D., and Harris, J. R., eds., Mineral and Energy Resource Assessment of the Greater Nahanni Ecosystem Under Consideration for the Expansion of the Nahanni National Park Reserve, Northwest Territories: Geological Survey of Canada, Open File 5344, p. 99–124.

Chung, C. F., and Fabbri, A., 2003, Validation of spatial prediction models for landslide hazards mapping: Nat. Hazards, v. 30, p. 451–472. doi:10.1023/B:NHAZ.0000007172.62651.2b.

Cline, J., Hofstra, A., Muntean, J., Tosdal, R. M., and Hickey, K. A., 2005,Carlin-type gold deposits in Nevada: critical geologic characteristics and viable models, *in* Hedenquist, W., Thompson, J. F. H., Goldfarb, R. J., and Richards, J. P., eds., Economic Geology 100th Anniversary Volume, Society of Economic Geologist, p. 451–484.

Cousens, B., 2007, Radiogenic isotope studies of Pb-Zn mineralization in the Howards Pass area, Selwyn Basin, *in* Wright, D. F., Lemkow, D., and Harris, J. R., Mineral and Energy Resource Assessment of the Greater Nahanni Ecosystem Under Consideration for the Expansion of the Nahanni National Park Reserve, Northwest Territories: Geological Survey of Canada, Open File 5344, p. 279–292.

Dawson, K. M., Panteleyev, A., Sutherland Brown, A., and Woodsworth, G. J., 1992, Regional Metallogeny, Chapter 19, *in* Gabrielse, H., and Yorath, C. J., eds., Geology of the Cordilleran Orogen in Canada: Geological Survey of Canada, Geology of Canada No. 4, p. 707–768 (also Geological Society of America, The Geology of North America, v. G2).

Day, S. J. A., Lariviere, J. M., Friske, P. W. B., Gochnauer, K. M., MacFarlane, K. E., McCurdy, M. W., and McNeil, R. J., 2005, National Geochemical Reconnaissance (NGR): regional stream sediment and water geochemical data, Macmillan Pass–Sekwi Mountains, Northwest Territories: Geological Survey of Canada, Open File 4949, 1 CD-ROM.

Department of Indian Affairs, Northern Development 2006, NORMIN.DB, The Northern Minerals Database: Northwest Territories Geoscience Office, Yellowknife, Northwest Territories.

Duk-Rodkin, A., Huntley, D., and Smith, R., 2007, Quaternary geology and glacial limits of the Nahanni National Park Reserve and adjacent areas, Northwest Territories, Canada, *in* Mineral and Energy Resource Assessment of the Greater Nahanni Ecosystem Under Consideration for the Expansion of the Nahanni National Park Reserve, Northwest Territories: Geological Survey of Canada, Open File 5344, p. 125–130.

Emsbo, P., Groves, D. I., Hofstra, A. H., and Bierlein, F. P., 2006, The giant Carlin gold province: a protracted interplay of orogenic, basinal, and hydrothermal processes above a lithospheric boundary: Miner. Deposita, v. 41, p. 517–525. doi:10.1007/s00126-006-0085-3.

Falck, H., 2007, Geological overview, Appenidx 1, *in* Wright, D. F., Lemkow, D., and Harris, J. R., eds., Mineral and Energy Resource Assessment of the Greater Nahanni Ecosystem Under Consideration for the Expansion of the Nahanni National Park Reserve, Northwest Territories: Geological Survey of Canada, Open File 5344, p. 327–365.

Friske, P. W. B., McCurdy, M. W., and Day, S. J. A., 2001, Regional stream sediment and water geochemical data, eastern Yukon and western Northwest Territories: Geological Survey of Canada, Open File 4016, 1 CD-ROM.

Goodfellow W. D., 2007, Mineral Deposits of Canada: Geological Association of Canada, MDD Special Paper 5, 1068 p.

Gordey, S. and Anderson, R. G., 1993, Evolution of the Northern Cordilleran Miogeocline, Nahanni Map Area (105I), Yukon and Northwest Territories: Geological Survey of Canada Memoir 428, 214 p.

Government of Canada, 1995, Terms of Reference, Mineral and Energy Resource Assessment (MERA) of Proposed National Parks in Northern Canada; commissioned and approved by the Senior MERA committee, Governments of Canada, Yukon and Northwest Territories, Ottawa; website http://www.nrcan.gc.ca/ms/pdf/merae.pdf.

Hamilton, S. M., Michel, F. A., Jefferson, C. W., and Power-Fardy, D., 2003, Spring water geochemistry and hydrogeology for mineral resource assessment of the South Nahanni River Region, *in* Jefferson C. W., and Spirito W., eds., Non-Renewable Mineral and Energy Resource Potential of the Proposed Extensions to Nahanni National Park Reserve, Northern Cordillera, Northwest Territories: Geological Survey of Canada, Open File 1686, p. 5-1 to 5-40.

Harris, J. R. and Sanborn-Barrie, M., 2006a, Mineral potential mapping: examples from the Red Lake Greenstone Belt, Northwest Ontario, *in* Harris, J. R., eds., GIS for the Earth Sciences: Geological Association of Canada, Special Volume 44, p. 1–21.

Harris, J. R., Sanborn-Barrie, M., Panagapko, D., Skulski, T., and Parker, J. R., 2006, Gold prospectivity maps of the Red Lake greenstone belt: application of GIS technology: Can. J. Earth Sci., v. 43, p. 865–893. doi:10.1139/E06-020.

Harris, J. R., Wilkinson, L., Heather, K., Fumerton, S., Bernier, M., and Dahn, R., 2001, Gold potential of the Swayze Greenstone Belt, Ontario: application of GIS technology: Nat. Resour. Res., v. 10, p. 91–124. doi:10.1023/A:1011548709573.

Jefferson, C. W., and Spirito, W. (eds.), 2003, Non-Renewable Mineral and Energy Resource Potential of the Proposed Extensions to Nahanni National Park Reserve, Northern Cordillera, Northwest Territories: Geological Survey of Canada, Open File 1686, 253 p.

Jefferson, C. W., Spirito, W. A., and Hamilton, S. M., 2003, Geological setting, Chapter 3, *in* Jefferson C. W., and Spirito, W., eds., Non-Renewable Mineral and Energy Resource Potential of the Proposed Extensions to Nahanni National Park Reserve, Northern Cordillera, Northwest Territories: Geological Survey of Canada, Open File 1686, p. 3-1 to 3-21.

Lariviere, J. M., Eddy, B. G., Udell, A., and Slack, T., 2006, Mackenzie Valley Mineral Potential Map; Northwest Territories Geoscience Office, Open File 2006–03, scale 1:1,500,000.

Lemkow, D., Harris, J. R., and Slack, T. (comp.), 2007, Digital geoscience database: a contribution to the mineral and energy resource assessment of the greater Nahanni ecosystem, Northwest Territories, Appendix 4, *in* Wright, D. F., ed., Mineral and Energy Resource Assessment of the Greater Nahanni Ecosystem Under Consideration for the Expansion of the Nahanni National Park Reserve, Northwest Territories.

Lydon, J., 1995, Sedimentary exhalative sulphides (SEDEX), *in* Eckstrand, O. R., Sinclair, W. D., and Thorpe, R. I., eds., Geology of Canadian Mineral Deposit Types No. 8: Geological Survey of Canada, p. 130–152 (also Geological Society of America, The Geology of North America, v. P-1).

McCurdy, M. W., McNeil, R. J., Friske, P. W. B., Day, S. J. B, Wilson, R. S., 2007, Stream sediment geochemistry in the proposed extension to the Nahanni Park Reserve, *in* Wright, D. F., Lemkow, D., and Harris, J., eds., Mineral and Energy Resource Potential of the Proposed Expansion to the Nahanni National Park Reserve, North Cordillera, Northwest Territories: Geological Survey of Canada, Open File 5344, p. 75–98.

Morrow, D. W., and Cook, D. G., 1987, The prairie creek embayment and lower paleozoic strata of the Southern Mackenzie Mountains: Geol. Surv. Canada, Memoir, v. 412, p. 195.

Morrow, D. W., Cumming, G. L., and Aulstead, K. L., 1990, The gas-bearing Devonian Manetoe Facies, Yukon and Northwest Territories: Geol. Surv. Canada, Bull., v. 400, p. 87.

Okulitch, A., 2005a, Geology of the Redstone River Area, National Earth Science Series, Geological Atlas: National Resources Canada, Map NP-9/10-G, scale 1:1 million.

Okulitch, A., 2005b, Geology of the Ross River Area, National Earth Science Series, Geological Atlas: National Resources Canada, scale 1:1 million.

Osadetz, K. G., Chen, Z., and Morrow, D. W., 2003, Petroleum resource assessment of the Tlogotsho Plateau, Nahanni Karst, and adjacent areas under consideration for expansion of Nahanni National Park Reserve, Northern Cordillera and District of Mackenzie, *in* Jefferson, C. W., and Spirito, W., eds., Non-Renewable Mineral and Energy Resource Potential of the Proposed Extensions to Nahanni National Park Reserve, Northern Cordillera, Northwest Territories: Geological Survey of Canada, Open File 1686, p. 8-1 to 8-36.

Paradis, S., 2007, Isotope geochemistry of the Prairie Creek carbonate-hosted zinc-lead-silver deposit, southern Mackenzie Mountains, Northwest Territories, *in* Wright, D. F., Lemkow, D., and Harris, J. R., eds., Mineral and Energy Resource Assessment of the Greater Nahanni Ecosystem Under Consideration for the Expansion of the Nahanni National Park Reserve, Northwest Territories: Geological Survey of Canada, Open File 5344, p. 131–176.

Plant, J. A., and Raiswell, R. W., 1994, Modifications to the geochemical signatures of ore deposits and their associated rocks in different surface environments, *in* Hale, M., and Plant, J. A., eds., Handbook of Exploration Geochemistry, v. 6: Drainage Geochemistry, Elsevier, p. 73–109.

Poulsen, K. H., 1996, Carlin-type gold deposits and their potential occurrence in the Canadian Cordillera, in Cordillera and Pacific Margin: Geological Survey of Canada, Current Research 1996-A, p. 1–9.

Rasmussen, K. L., Mortensen, J. K., and Falck, H., 2006, Morphological and compositional analysis of placer gold in the South Nahanni River drainage, Northwest Territories: Yukon Explor. Geol., v. 2006, p. 237–250.

Rasmussen, K. L., Mortensen, J. K., Falck, H. and Ullrich, T. D., 2007, The potential for intrusion-related mineralization within the South Nahanni River MERA area, Selwyn and Mackenzie Mountains, Northwest Territories, *in* Wright, D. F., Lemkow, D., and Harris, J. R., eds., Mineral and Energy Resource Assessment of the Greater Nahanni Ecosystem Under Consideration for the Expansion of the Nahanni National Park Reserve, Northwest Territories: Geological Survey of Canada, Open File 5344, p. 203–278.

Richards, B. G., 1989, Report on the Selena Creek placer property, Nahanni Mining Division, Northwest Territories, Latitude: 60°55'N; Longitude: 126°40'W; unpub. report for Sirius Resource Corporation and Verdstone Gold Corporation; Dynamin Engineering Limited, Vancouver, 19 p.

Rowan, L., 1989, Similarities of geological environment and potential for Carlin-style mineralization at Selena Creek; INAC Assessment Files, November 27, 1989, unpub. memorandum.

Spirito, W. A. and Jefferson, C. W., 2003, Regional surficial geochemistry, *in* Jefferson, C. W., and Spirito, W., eds., Non-Renewable Mineral and Energy Resource Potential of the Proposed Extensions to Nahanni National Park Reserve, Northern Cordillera, Northwest Territories: Geological Survey of Canada, Open File 1686, p. 4-1 to 4-79.

Wright D. F., Bonham-Carter G. F., 1996, VHMS favourability mapping with GIS-based integration models, Chisel Lake-Anderson Lake area, *in* Bonham-Carter, G. F., Galley, A. G., Hall, G. E. M. (eds.) EXTECH I: A multidisciplinary approach to massive sulphide research in the Rusty Lake-Snow Lake Greenstone Belts, Manitoba: Geological Survey of Canada, Bulletin 426, p. 339–376.

Yuvan, J., Shelton, K., and Falck, H., 2007, Geochemical investigations of the high-grade quartz, *in* Wright, D. F., Lemkow, D., and Harris, J. R., eds., Mineral and Energy Resource Assessment of the Greater Nahanni Ecosystem Under Consideration for the Expansion of the Nahanni National Park Reserve, Northwest Territories: Geological Survey of Canada, Open File 5344, p. 177–190.